Outputbased enhanced closedloop model reference adaptive control and its application to direct yaw moment control

Received: 22 July 2023 | Revised: 19 February 2024 | Accepted: 23 May 2024

DOI: 10.1002/rnc.7471

RESEARCH ARTICLE

WILEY

Output-based enhanced closed-loop model reference adaptive control and its application to direct yaw moment control

Umberto Montanaro[1] | **Chen Chen**[1,2] | **Alessandro Rizzo**[3,4] | **Aldo Sorniotti**[5]

[1]School of Mechanical Engineering Sciences, University of Surrey, Guildford, Surrey, UK

[2]Department of Energy "Galileo Ferraris", Politecnico di Torino, Turin, Italy

[3]Department of Electronics and Telecommunications, Politecnico di Torino, Turin, Italy

[4]Office of Innovation, Tandon School of Engineering, New York University, Brooklyn, New York, USA

[5]Department of Mechanical and Aerospace Engineering (DIMEAS), Politecnico di Torino, Turin, Italy

Correspondence
Umberto Montanaro, School of Mechanical Engineering Sciences, University of Surrey, Guildford, Surrey GU2 7XH, UK.
Email: u.montanaro@surrey.ac.uk

Abstract

The enhanced model reference adaptive control (EMRAC) algorithm is an effective full-state adaptive solution to control plants affected by nonlinear unmodelled dynamics and persistent disturbances. The EMRAC strategy improves the tracking performance by equipping the MRAC algorithm with adaptive switching and adaptive integral control actions. However, the need for the plant state prevents the applicability of the EMRAC algorithm to engineering control problems where only the plant output is measurable. To cover this gap and extend the range of plants controllable by EMRAC solutions, this article presents an output-based EMRAC algorithm leveraging the closed-loop (CL) MRAC formulation. The robustness of the closed-loop control system is analytically analysed, not only with respect to plant parameter uncertainties and square measurable disturbances, but also to $\mathcal{L}_\infty$ unmodelled terms and disturbances. The ultimate boundedness of the closed-loop control system is assessed with respect to $\mathcal{L}_\infty$ unknown nonlinear terms and disturbances, by using Lyapunov theory for Filippov systems, as the adaptive switching control action makes the closed-loop system discontinuous. To assess the effectiveness of the CL-EMRAC strategy to impose reference trajectories despite the unmodelled plant dynamics and persistent bounded disturbances, the problem of vehicles' direct yaw moment control is used as an engineering case study. The closed-loop tracking performance is also quantitatively evaluated through a set of key performance indicators and compared to those provided by four benchmark controllers, that is, two LQ-based strategies and two MRAC-based control solutions. The CL-EMRAC and benchmark controllers are implemented and tested in a co-simulation environment based on a high-fidelity IPG CarMaker vehicle model.

KEYWORDS

adaptive robust control systems, closed-loop MRAC, direct yaw moment control

1 | INTRODUCTION

Enhanced model reference adaptive control (EMRAC) strategies are effective control solutions to impose the reference model dynamics to plants despite parameter uncertainties, unmodelled plant dynamics, and disturbances. EMRAC solutions improve the tracking performance obtainable through the MRAC technique by adding an adaptive integral action and an adaptive switching control action. Engineering control applications that have been tackled through EMRAC solutions include automotive electromechanical valves,[1] multi-enclosed thermal zones,[2] path following control for autonomous vehicles[3] and robotic manipulators,[4] just to name a few. In Reference 1, the EMRAC closed-loop tracking performance was experimentally compared to those provided by other robust adaptive solutions and classical MRAC techniques, and it was shown that the additional EMRAC control actions are vital for improving the tracking of the reference dynamics. However, the available EMRAC solutions are full-state feedback control algorithms. The hypothesis of having the plant state accessible is a limitation for the EMRAC applicability to engineering problems where only a subset of states is measurable, for example, in the cases where some states are not measured for avoiding expensive sensors. An empirical adjustment to the EMRAC algorithm for operating the controller with a reduced number of states has been experimentally tested in Reference 1, where the adaptive gain for the non-measurable state was locked to zero. However, an output-based EMRAC strategy with a consistent analytical analysis of the closed-loop dynamics is still not available. To cover this gap in the EMRAC literature, this article presents, to the best of the authors' knowledge, the first output-based formulation of the EMRAC algorithm by exploring a closed-loop reference model approach and the related analysis of the closed-loop system. The theory of closed-loop model reference adaptive control is still relatively new when compared to the classical MRAC approaches,[5] as initial attempts to modify the reference model dynamics with the use of tracking errors were presented less than two decades ago.[6]

The idea underpinning the closed-loop model reference adaptive control theory is the modification of the reference model with a proportional feedback term based on the tracking error. The proportional feedback gain is an additional control gain that, for instance, can be used to reduce oscillations in the state and input, and, as a consequence, to improve the transient dynamics.[6] Furthermore, the proportional feedback action enables the use of the reference model as an observer. This allows the design of adaptive solutions where the reference model state replaces the plant state in the computation of the control action, thus paving the way to output-based closed-loop MRAC solutions.[7] However, the benefits obtained by adjusting the reference system with the output tracking error come at the cost that the actual reference dynamics might deviate considerably from the desired ones, specified by the open-loop part of the reference model, if large residual errors persist, for example, because of persistent disturbances. Consequently, robust terms should be included in the closed-loop model reference adaptive control approaches to shrink the residual error also in the presence of $\mathcal{L}_\infty$ unmodelled dynamics and disturbances. In this article, an output-based control solution based on the EMRAC formulation, denoted as CL-EMRAC strategy, is proposed and the robustness to persistent unwanted dynamics and disturbances is achieved through: *(i)* the adaptive integral and switching control actions, which improve the convergence of the tracking error despite unmodelled offsets, disturbances, and bounded nonlinear unmodelled terms; and *(ii)* the use of the switching σ-modification strategy in the adaptation laws, which prevents the unbounded growth of the adaptive gains if they exceed a given threshold because of the unmodelled dynamics and disturbances.

Recent studies in the field of MRAC solutions with closed-loop reference model include extensions of this theory to switched systems[8]; plants with actuator failures[9,10]; networks of dynamic systems[11]; and cyber-physical systems to improve resilience to false data injection attacks.[12] Furthermore, in Reference 13 an adaptive control term expressed as a linear regression of the adaptive gains, known plant nonlinearities and filtered versions of the plant state and control action is used in the formulation of an MRAC algorithm with a closed-loop reference model. The resulting control action improves the transient and steady-state responses also in the presence of large feedback gains used for modifying the reference model dynamics that help to achieve faster convergence of the tracking error. Filter versions of adaptive control gains are also used in Reference 14 in conjunction with a parameter projection method for the design of a closed-loop MRAC scheme, which is also able to provide bounded tracking error for non-parametric uncertainties. However, the solutions in References 13 and 14 are full state-feedback strategies, thus they can be used only when all plant states are measurable. In Reference 15, a reinforcement learning strategy is proposed to adjust online the feedback gain of the reference model dynamics to improve the transient response performance of the closed-loop adaptive control system. However, unmatched uncertainties have not been considered in the formulation of the plant dynamics, which potentially could degrade the closed-loop tracking performance and induce unbounded drifting in the evolution of the adaptive control gains. An output-based solution has been proposed in Reference 16, where the controller design combines open-loop and

closed-loop reference models. Specifically, the open-loop reference model is used to generate the reference dynamics, while the closed-loop reference model is adopted as an observer. The control solution in Reference 16 was shown to provide lower tracking error, and more closely tracks the output of the reference model, when compared to the classical closed-loop MRAC algorithm, but at the cost of slightly higher oscillations.

However, MRAC solutions with closed-loop reference models equipped with adaptive switching and integral actions to systematically counteract disturbances and unmodelled dynamics, thus improving the tracking performance and the convergence of the dynamics towards desired ones independently from the magnitude of the feedback gain, have not been presented in the literature.

In this article, the closed-loop system obtained with the novel CL-EMRAC algorithm is analytically and systematically studied for different classes of disturbances. The closed-loop dynamics are proven to be globally uniformly ultimately bounded for matched and unmatched $\mathcal{L}_\infty$ unmodelled dynamics and disturbances, and the effect of the switching control action on the ultimate bound is analysed. The ultimate boundedness of the closed-loop dynamics requires that the tracking error is attracted and stays confined in an n-dimensional sphere centered in the origin despite of unmatched disturbances or unmodelled nonlinear dynamics often occurring in engineering applications.[17]

Furthermore, conditions for the asymptotic convergence of the tracking error are also investigated for $\mathcal{L}_2$ and $\mathcal{L}_\infty$ disturbances. However, as the switching control action included in the CL-EMRAC makes the closed-loop system non-smooth, results available for controlling nonlinear systems with Lipschitz vector fields, for example, in References 18 and 17, cannot be applied, thus the extensions of Lyapunov theory to Filippov systems in Reference 19 are exploited for assessing the closed-loop ultimate boundedness. An overview of the Filippov theory for studying of the ultimate boundedness of discontinuous systems can be found in Appendix A.[4]

To show the effectiveness of the novel output-based CL-EMRAC algorithm to control nonlinear plants of engineering interest, the direct yaw moment control (DYC) problem[20] of vehicles is selected as a case study. DYC systems are used in modern vehicles to improve the cornering performance, that is, to shape the under-steer characteristics in quasi-steady-state conditions and to enhance stability in severe transient maneuvers. The idea behind DYC systems is to track a reference yaw rate by using a control yaw moment that is generated by adjusting the asymmetrical distribution of longitudinal tire forces among the wheels. Robust yaw rate control is a challenging task because of the combination of several factors, such as: *(i)* vehicle nonlinearities, for example, nonlinear tire dynamics; *(ii)* difficulties to estimate system parameters such as the tire-road friction coefficient; *(iii)* dependence of the lateral vehicle dynamics on vehicle speed; *(iv)* external disturbances (e.g., wind gusts and banking angle); and *(v)* varying vehicle parameters such as the vehicle mass and mass moments of inertia.

MRAC strategies for DYC systems have been investigated to tackle the aforementioned challenges, for example, in References 21–25. In Reference 21, a set of MRAC DYC solutions have been designed and compared for different tire-road friction conditions. In Reference 22, an indirect MRAC algorithm has been proposed, where the adaptive feedback control action is augmented with an integral control strategy to improve the tracking performance of the reference yaw rate for an in-wheel electric vehicle, in presence of vehicle parameters uncertainties. In Reference 26, the yaw rate control has been used as a test case for an MRAC algorithm for piecewise smooth systems. Specifically, the nonlinear lateral tire force characteristics are linearized into three regions of the tire slip angle, and the reference yaw rate is imposed to the resulting piecewise affine system via a hybrid MRAC, despite the vehicle parameter uncertainties. In References 23 and 24, an MRAC strategy is formulated for concurrently controlling the direct yaw moment and an active front steering system for enhancing vehicle handling and stability, by imposing a reference yaw rate and sideslip angle. In Reference 25, an MRAC-based DYC system is devised, and it is shown that the resulting yaw rate tracking performance outperforms those provided by a sliding mode strategy for different tire-road friction conditions, without any chattering on the control action. Although they are effective, the previous adaptive control strategies are full-state feedback control solutions, which require the use of the vehicle sideslip angle. However, vehicle sideslip can be only estimated in production vehicles, as sideslip angle sensors are costly and can be used exclusively for research purposes.[27] Consequently, robust output-based MRAC strategies are desirable, but, to the best of the authors' knowledge, output-based closed-loop MRAC solutions for controlling the vehicle yaw rate through DYC have been only marginally investigated. An output-based closed-loop MRAC algorithm has been recently designed in Reference 28 for path-tracking control, where the steering wheel angle is the control input rather than a measurable disturbance as in the case of typical DYC systems.

In this article, the novel output-based CL-EMRAC strategy is used for the DYC problem. The resulting controller is implemented in a high-fidelity co-simulation environment based on IPG CarMaker.

In summary, the contributions of this article are:

- an extension of the EMRAC algorithms via the design of a novel output-based EMRAC strategy leveraging a closed-loop reference model formulation along with the analysis of the closed-loop system stability and ultimate boundedness for different classes of disturbances, for example, unmatched disturbances. Hence, from a theory viewpoint the proposed algorithm *(i)* enlarges the applicability of the EMRAC strategies to engineering plants where only the plant output is measurable, and *(ii)* increases the robustness of MRAC algorithms with closed-loop reference models thought the use of the additional adaptive control actions characterizing EMRAC strategies;
- the application of the novel CL-EMRAC strategy to the DYC problem without the use of the sideslip angle feedback.

The effectiveness of the proposed control solution to steer the vehicle dynamics towards the reference ones is shown through an objective simulation-based comparison of the closed-loop tracking performance provided by the CL-EMRAC strategy with those of four benchmark controllers, that is, the linear quadratic regulator (LQR) and the robust LQR (RLQR) in Reference 29, the basic MRAC algorithm in Reference 30, and the output-based closed-loop MRAC (CL-MRAC) strategy obtained by removing from the CL-EMRAC the adaptive integral and adaptive switching control actions (i.e., the robust actions). The comparison between the CL-EMRAC algorithm and the benchmark control solutions is quantitatively carried out via a set of key performance indexes (KPIs) relevant for direct yaw moment control systems.[29]

In the rest of the article, $\mathcal{I}_n$ is the identity matrix in $\mathbb{R}^{n\times n}$ while $\mathcal{O}_{n,m}$ denotes the zero matrix in $\mathbb{R}^{n\times m}$. Given a symmetric matrix $\mathcal{Q}\in\mathbb{R}^{n\times n}$, then $\lambda_{\min}(\mathcal{Q})$ and $\lambda_{\max}(\mathcal{Q})$ are the minimum and the maximum eigenvalue of $\mathcal{Q}$, respectively. For a sequence of matrices $\mathcal{Q}_j\in\mathbb{R}^{n_j\times n_j}$, with $j=1,\ \dots\ ,m$, $\Delta(\mathcal{Q}_1,\mathcal{Q}_2,\ \dots\ ,\mathcal{Q}_m)$ denotes the block diagonal matrix in $\mathbb{R}^{(n_1+\cdots+n_m)\times(n_1+\dots+n_m)}$ with $\mathcal{Q}_j$ being the jth block. Moreover, a dynamic system is uniformly ultimately bounded with ultimate bound $\epsilon_{ub}>0$ when for the system solutions $\widetilde{x}(t)$ there exists a $\mathcal{KL}$-function $\Psi:\mathbb{R}^+\times\mathbb{R}^+\to\mathbb{R}^+$ such that

$$\|\widetilde{x}(t)\|\leq\Psi\big(\widetilde{x}(t_0),t-t_0\big),\ \forall\ t_0\leq t\leq t_0+\mathcal{T},\quad\text{and}\quad\|\widetilde{x}(t)\|\leq\epsilon_{ub},\ \forall\ t\geq t_0+\mathcal{T}. \tag{1}$$

with t_0 and $\mathcal{T}$ being the system initial time instant and a time interval (dependent on $\widetilde{x}(t_0)$), respectively.

The remainder is organized as follows. Section 2 presents the CL-EMRAC strategy, while Section 3 analyses the closed-loop system, and provides the proof of the closed-loop stability and ultimate boundedness. The CL-EMRAC design for the DYC problem is discussed in Section 4. The simulation results and the comparison with benchmark controllers are presented in Section 5, while conclusions are drawn in Section 6. Appendices A and B present the proofs of the lemmas used to support the closed-loop system analysis.

2 | THE CLOSED-LOOP EMRAC ALGORITHM

Consider the plant model of the form

$$\dot{x}=Ax+Bu+Ed+\mathcal{G},\quad x(t_0)=x_0, \tag{2a}$$

$$y=Cx, \tag{2b}$$

where $x\in\mathbb{R}^{n_x}$ is the plant state, $u\in\mathbb{R}$ is the control input, $y\in\mathbb{R}^{n_y}$ is the system output, $d\in\mathbb{R}^{n_d}$ is a bounded measurable disturbance (i.e., there exists d_∞, such that $\|d(t)\|<d_\infty$, $\forall\ t\geq t_0$), $\mathcal{G}\in\mathbb{R}^{n_x}$ is a non-measurable disturbance which parametrization will be presented later, n_x, n_y and n_d are the dimension of the state, output and measurable disturbance, respectively, while t_0 is the initial time and $x_0\in\mathbb{R}^{n_x}$ is the initial state. Moreover, $A\in\mathbb{R}^{n_x\times n_x}$, $B\in\mathbb{R}^{n_x}$, $E\in\mathbb{R}^{n_x\times n_d}$ and $C\in\mathbb{R}^{n_y\times n_x}$ are the dynamic matrix, the input matrix, the output matrix and the matrix of the measurable disturbance, respectively. The matrices of the dynamic model (2a) are supposed to have unknown constant entries, while the output matrix is known. System (2) is often adopted for the formulation of control oriented models of plants of engineering interest to enable the systematic design of effective control strategies, and accounts for *(i)* linear contributions to the state evolution (e.g., obtained by linearizing nonlinear plant models or the application of feedback linearization strategies); *(ii)* an unknown disturbance term for representing residual unmodelled nonlinear dynamics and external non-measurable disturbances; and *(iii)* measurable disturbances (e.g., for modeling system inputs that are measurable but not manipulable).

The control target for the CL-EMRAC is to steer the plant dynamics (2) towards those of the following reference model

$$\dot{x}_m = A_m x_m + B_m r + E_m d + L(y_m - y), \quad x_m(t_0) = x_{m0}, \tag{3a}$$

$$y_m = C x_m, \tag{3b}$$

where $x_m \in \mathbb{R}^{n_x}$ is the state of the reference model, $x_{m0} \in \mathbb{R}^{n_x}$ is the initial reference model state, while $y_m \in \mathbb{R}^{n_y}$ and $r \in \mathbb{R}$ are the reference output and the bounded reference input, respectively. Furthermore, $A_m \in \mathbb{R}^{n_x \times n_x}$, $B_m \in \mathbb{R}^{n_x}$ and $E_m \in \mathbb{R}^{n_x \times n_d}$ are the dynamic matrix, the input matrix and the matrix of the measurable disturbance of the reference model, respectively. The matrix $L \in \mathbb{R}^{n_x \times n_y}$ is the proportional gain for the feedback term in reference model dynamics which will be designed later.

The non-measurable disturbance is assumed to be parametrized as

$$\mathcal{G} = B_m g + \widehat{\mathcal{G}} + E_v v, \tag{4}$$

where $g \in \mathbb{R}$ and $\widehat{\mathcal{G}} \in \mathbb{R}^{n_x}$ are bounded disturbances (i.e., g and $\widehat{\mathcal{G}} \in \mathcal{L}_\infty$, thus there exist known constants $g_\infty > 0$ and $\widehat{\mathcal{G}}_\infty > 0$, such that $\|g(t)\| \le g_\infty$ and $\|\widehat{\mathcal{G}}(t)\| \le \widehat{\mathcal{G}}_\infty, \forall\, t \ge t_0$), $v \in \mathbb{R}^{n_v}$ is an unknown bounded square-measurable disturbance (i.e., $v \in \mathcal{L}_\infty \cap \mathcal{L}_2$) and $E_v \in \mathbb{R}^{n_x \times n_v}$ is a known disturbance matrix with n_v being the dimension of the disturbance v. Notice that, also the resulting disturbance $\mathcal{G}$ in (4) is bounded, thus there exists a constant $\mathcal{G}_\infty > 0$ such that $\|\mathcal{G}(t)\| \le \mathcal{G}_\infty, \forall\, t \ge t_0$.

Assumption 1. There exist some constant vectors $\widehat{\phi}_X \in \mathbb{R}^{n_x}$, $\widehat{\phi}_D \in \mathbb{R}^{n_d}$ and $\widehat{\phi}_R \in \mathbb{R}$, such that

$$B_m = B\widehat{\phi}_R, \quad A_m = A + \frac{1}{\widehat{\phi}_R} B_m \widehat{\phi}_X^T, \text{ and } E_m = E + \frac{1}{\widehat{\phi}_R} B_m \widehat{\phi}_D^T. \tag{5}$$

Assumption 2. The sign of $\widehat{\phi}_R$ is known and there exist known positive constants, $\widehat{\phi}_{R,l}$, $\widehat{\phi}_{R,u}$, $\widehat{\phi}_{X,u}$ and M_ϕ such that

$$\widehat{\phi}_{R,l}^2 < \left|\widehat{\phi}_R\right|^2 < \widehat{\phi}_{R,u}^2, \tag{6a}$$

$$\widehat{\phi}_{X,u}^2 \ge \left\|\widehat{\phi}_X\right\|^2, \tag{6b}$$

$$M_\phi > \|\widehat{\phi}\|, \tag{6c}$$

with

$$\widehat{\phi} = \begin{bmatrix} \widehat{\phi}_X^T & \widehat{\phi}_R & \widehat{\phi}_D^T & \widehat{\phi}_I^T \end{bmatrix}^T = \begin{bmatrix} \widehat{\phi}_R B_m^\dagger (A_m - A) & B B_m^\dagger & \widehat{\phi}_R B_m^\dagger (E_m - E) & \mathcal{O}_{n_x}^T \end{bmatrix}^T, \tag{7}$$

where $B_m^\dagger = B_m^T \left(B_m B_m^T\right)^{-1}$ and $\widehat{\phi}_I^T = \mathcal{O}_{n_x}^T$.

Assumption 3. For given constants $\theta > \theta^\star$ and $\Gamma_N = \Gamma_N^T > 0$ belonging to $\mathbb{R}^{n_y \times n_y}$, there exist $\varepsilon > 0$, $\Omega \in \mathbb{R}^{n_x \times n_y}$ and $H \in \mathbb{R}^{n_y}$, and strictly positive definite matrices $P, Q \in \mathbb{R}^{n_x \times n_x}$, such that

$$\Pi = \begin{bmatrix} PA_m + A_m^T P + \Omega C + C^T \Omega^T + \mathcal{I}_{n_x} & \mathcal{I}_{n_x} & C^T \Gamma_N H & P\widetilde{E}_v \\ * & -Q^{-1} & \mathcal{O}_{n_x} & \mathcal{O}_{n_x, \tilde{n}_v} \\ * & * & -\theta^{-1}/2 & \mathcal{O}_{1, \tilde{n}_v} \\ * & * & * & -\varepsilon^2 \mathcal{I}_{\tilde{n}_v} \end{bmatrix} < 0, \tag{8}$$

$$\theta^\star = \frac{\widehat{\phi}_{X,u}^2}{2\widehat{\phi}_{R,l}^2} \max\left\{1, \frac{1}{\lambda_{\min}(Q)}\right\}, \tag{9}$$

$$PB_m = C^T \Gamma_N H, \tag{10}$$

with

$$\widetilde{E}_v = \begin{cases} E_v, & \text{if } E_v \neq 0, \\ \mathcal{O}_{n_x}, & \text{if } E_v = 0, \end{cases} \quad \text{and} \quad \tilde{n}_v = \begin{cases} n_v, & \text{if } E_v \neq 0, \\ 1, & \text{if } E_v = 0. \end{cases} \tag{11}$$

Based on Assumption 3, the output feedback control gain L in (3) is set as

$$L = P^{-1}\Omega. \tag{12}$$

The CL-EMRAC strategy computes the control action as

$$u(t) = u_{\text{CL-MRAC}}(t) + u_D(t) + u_I(t) + u_N(t), \tag{13}$$

with

$$u_{\text{CL-MRAC}}(t) = K_X(t)x_m(t) + K_R(t)r(t), \tag{14a}$$

$$u_D(t) = K_D(t)d(t), \tag{14b}$$

$$u_I(t) = K_I(t)y_I(t), \tag{14c}$$

$$u_N(t) = K_N(t)q_N(y_e(t)), \tag{14d}$$

where the output tracking error $y_e \in \mathbb{R}^{n_y}$ is defined as

$$y_e = y_m - y, \tag{15}$$

and $y_I \in \mathbb{R}^{n_y}$ is the integral of the output tracking error whose dynamics are computed as

$$\dot{y}_I = y_e - \sigma_I(\|y_I\|)\rho_e y_I, \tag{16}$$

where $\rho_e \in \mathbb{R}^{n_y \times n_y}$ is a diagonal strictly positive matrix, and $\sigma_I(\|y_I\|)$ is a σ-modification function defined as

$$\sigma_I(\|y_I\|) = \begin{cases} 0 & \text{if } \|y_I\| \leq \widehat{M}_I, \\ \eta_I\left(\frac{\|y_I\|}{\widehat{M}_I} - 1\right) & \text{if } \widehat{M}_I < \|y_I\| \leq 2\widehat{M}_I, \\ \eta_I & \text{if } \|y_I\| > 2\widehat{M}_I, \end{cases} \tag{17}$$

with $\widehat{M}_I$ and η_I being strictly positive constants.

The discontinuous term $q_N(y_e)$ in (14d) is defined as

$$q_N(y_e) = \text{sgn}(H^T\Gamma_N y_e), \tag{18}$$

with $\Gamma_N \in \mathbb{R}^{n_y \times n_y}$ being the strictly positive matrix in Assumption 3.

The adaptive gains in (14) are updated in accordance with the following adaptive laws

$$K_X = \phi_X^T + H^T\Gamma_N y_e x_m^T \beta_X, \quad \text{and} \quad \dot{\phi}_X^T = H^T\Gamma_N y_e x_m^T \alpha_X + f_X^T, \tag{19a}$$

$$K_R = \phi_R + H^T\Gamma_N y_e r \beta_R, \quad \text{and} \quad \dot{\phi}_R = H^T\Gamma_N y_e r \alpha_R + f_R, \tag{19b}$$

$$K_D = \phi_D^T + H^T\Gamma_N y_e d^T \beta_D, \quad \text{and} \quad \dot{\phi}_D^T = H^T\Gamma_N y_e d^T \alpha_D + f_D^T, \tag{19c}$$

$$K_I = \phi_I^T + H^T \Gamma_N y_e y_I^T \beta_I, \quad \text{and} \quad \dot{\phi}_I^T = H^T \Gamma_N y_e y_I^T \alpha_I + f_I^T, \tag{19d}$$

$$K_N = \phi_N, \quad \text{and} \quad \dot{\phi}_N = \alpha_N h_N\left(\|y_e\|_\Theta\right) + f_N, \tag{19e}$$

where $\alpha_X, \beta_X, \alpha_I, \beta_I \in \mathbb{R}^{n_x \times n_x}$, $\alpha_D, \beta_D \in \mathbb{R}^{n_d \times n_d}$ and $\alpha_N, \alpha_R, \beta_R \in \mathbb{R}$ are diagonal matrices with diagonal entries having the same sign of $\widehat{\phi}_R$, $\|y_e\|_\Theta = y_e^T \Theta y_e$, with $\Theta \in \mathbb{R}^{n_y \times n_y}$ being a positive matrix and

$$h_N\left(\|y_e\|_\Theta\right) = \frac{\|y_e\|_\Theta^{c_3}}{c_1 + c_2 \|y_e\|_\Theta^{c_3}}, \tag{20}$$

where c_1, c_2 and c_3 are positive constants.

The terms $f_X, f_I \in \mathbb{R}^{n_x}$, $f_R, f_N \in \mathbb{R}$ and $f_D \in \mathbb{R}^{n_d}$ are the leakage factors of the adaptive mechanism and are used as locking strategies for preventing the unbounded evolution of the integral part of the adaptive gains (19) in the presence of persistent disturbances and unmodelled dynamics and are computed as

$$f_X^T = -\sigma_\phi(\|\phi\|)\phi_X^T \rho_X, \quad f_R = -\sigma_\phi(\|\phi\|)\phi_R \rho_R, \quad f_D^T = -\sigma_\phi(\|\phi\|)\phi_D^T \rho_D, \quad f_I^T = -\sigma_\phi(\|\phi\|)\phi_I^T \rho_I, \tag{21a}$$

$$f_N = -\sigma_N(\|\phi_N\|)\phi_N \rho_N, \tag{21b}$$

where $\rho_X, \rho_I \in \mathbb{R}^{n_x \times n_x}$, $\rho_D \in \mathbb{R}^{n_d \times n_d}$, and $\rho_N, \rho_R \in \mathbb{R}$ are strictly positive matrices and the vector $\phi \in \mathbb{R}^{n_w}$ is the vector collecting the integral part of the adaptive gains in (19a)–(19d), that is,

$$\phi = \begin{bmatrix} \phi_X^T & \phi_R & \phi_D^T & \phi_I^T \end{bmatrix}^T = \begin{bmatrix} \phi_1 & \phi_2 & \cdots & \phi_{n_w - 1} & \phi_{n_w} \end{bmatrix}^T, \tag{22}$$

where $\phi_j, j = 1, \ldots, n_w$, is the jth entry of ϕ and $n_w = 2n_x + n_d + 1$.

The σ-modification function $\sigma_\phi(\|\phi\|)$ is defined as

$$\sigma_\phi(\|\phi\|) = \begin{cases} 0, & \text{if } \|\phi\| \le \widehat{M}_\phi, \\ \eta_\phi\left(\frac{\|\phi\|}{\widehat{M}_\phi} - 1\right), & \text{if } \widehat{M}_\phi < \|\phi\| \le 2\widehat{M}_\phi, \\ \eta_\phi, & \text{if } \|\phi\| > 2\widehat{M}_\phi, \end{cases} \tag{23}$$

where $\widehat{M}_\phi$ and η_ϕ are strictly positive constants such that

$$\frac{\eta_\phi}{\widehat{\phi}_R} \lambda_{\min}\left(\Gamma_\rho \Gamma_\alpha^{-1}\right) > \frac{3}{4} \lambda_{\min}(Q), \tag{24}$$

$$\widehat{M}_\phi \ge \sqrt{\frac{\lambda_{\max}\left(\operatorname{sgn}\left(\widehat{\phi}_R\right)\Gamma_\rho \Gamma_\alpha^{-1}\right)}{\lambda_{\min}\left(\operatorname{sgn}\left(\widehat{\phi}_R\right)\Gamma_\rho \Gamma_\alpha^{-1}\right)}} M_\phi, \tag{25}$$

where the matrices $\Gamma_\alpha \in \mathbb{R}^{n_w \times n_w}$ and $\Gamma_\rho \in \mathbb{R}^{n_w \times n_w}$ are defined as

$$\Gamma_\alpha = \Delta(\alpha_X, \alpha_R, \alpha_D, \alpha_I) = \operatorname{diag}\left(\alpha_1, \alpha_2, \ldots, \alpha_{n_w}\right), \tag{26}$$

$$\Gamma_\rho = \Delta(\rho_X, \rho_R, \rho_D, \rho_I) = \operatorname{diag}\left(\rho_1, \rho_2, \ldots, \rho_{n_w}\right), \tag{27}$$

with α_j, and $\rho_j, j = 1, \ldots, n_w$, are the jth entry on the diagonal of Γ_α and Γ_ρ, respectively.

The σ-modification function $\sigma_N(\|\phi_N\|)$ is

$$\sigma_N(\|\phi_N\|) = \begin{cases} 0, & \text{if } \|\phi_N\| \leq \widehat{M}_N, \\ \eta_N\left(\frac{\|\phi_N\|}{\widehat{M}_N} - 1\right), & \text{if } \widehat{M}_N < \|\phi_N\| \leq 2\widehat{M}_N, \\ \eta_N, & \text{if } \|\phi_N\| > 2\widehat{M}_N, \end{cases} \tag{28}$$

where η_N and $\widehat{M}_N$ are strictly positive constants and

$$\widehat{M}_N > g_\infty \widehat{\phi}_{R,u}. \tag{29}$$

The formulation of the main theorem for the CL-EMRAC requires the definition of the following closed-loop states

$$x_e = x_m - x, \quad \phi_e = \widehat{\phi} - \phi, \quad \text{and} \quad \widetilde{x}_e = \begin{bmatrix} x_e^T & \phi_e^T \end{bmatrix}^T, \tag{30}$$

along with the following constants and functions

$$\widetilde{P} = \Delta\left(P, \frac{1}{\widehat{\phi}_R}\Gamma_\alpha^{-1}\right) \in \mathbb{R}^{(n_x+n_w)\times(n_x+n_w)}, \tag{31}$$

$$\mu_1 = \frac{3}{4}\lambda_{\min}(Q), \quad \mu_2\left(\widetilde{\mathcal{G}}_\infty\right) = \frac{3\|P\|^2\widetilde{\mathcal{G}}_\infty^2}{\mu_1} + \mu_1\left(2\widehat{M}_\phi + \|\widehat{\phi}\|\right)^2, \quad \mu\left(\widetilde{\mathcal{G}}_\infty\right) = \sqrt{\frac{\mu_2\left(\widetilde{\mathcal{G}}_\infty\right)}{\mu_1(1-\zeta)}}, \tag{32}$$

with $\zeta \in (0,\ 1)$, and

$$\widetilde{\mathcal{G}}_\infty^2 = \begin{cases} \widehat{\mathcal{G}}_\infty^2, & \text{if } gB_m^T\widehat{\mathcal{G}} \geq 0, \ \forall\, t \geq t_0, \\ \mathcal{G}_\infty^2, & \text{otherwise.} \end{cases} \tag{33}$$

A schematic of the output-based CL-EMRAC strategy is shown in Figure 1.

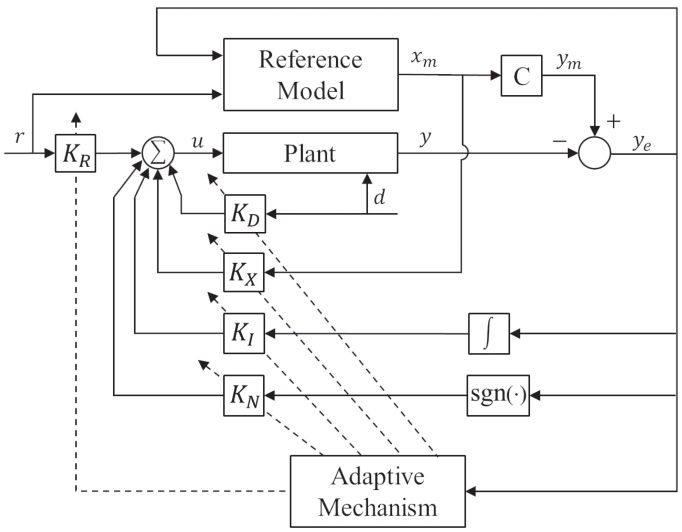

FIGURE 1 Output-based CL-EMRAC scheme.

Theorem 1. *Given system (2) and the closed-loop reference model (3), if Assumptions 1 to 3 are fulfilled, then the CL-EMRAC strategy (13) equipped with the adaptive mechanism (19) guarantees the boundedness of all closed-loop signals. Furthermore,*

(a) if $\widehat{\mathcal{G}} \neq 0$ and $E_v = 0$ (or equivalently the square-measurable disturbance v is zero), the dynamics of the state tracking error are globally uniformly ultimately bounded. Moreover, there exists a time interval $\mathcal{T}$ (dependent on $\widetilde{x}_e(t_0)$) such that

$$||\widetilde{x}_e(t)|| \leq \sqrt{\frac{\lambda_{max}(\widetilde{P})}{\lambda_{min}(\widetilde{P})}}\mu(\widetilde{\mathcal{G}}_\infty), \quad \forall\, t \in [t_0 + \mathcal{T}, +\infty), \tag{34}$$

where $\widetilde{P}$ is the strictly positive matrix defined in (31) and $\mu(\widetilde{\mathcal{G}}_\infty)$ is computed in accordance with (32).

(b) if $\widehat{\mathcal{G}} = 0$ and $E_v = 0$ (or equivalently the square-measurable disturbance v is zero), then the state of system (2) asymptotically tracks that of the reference model (3), that is,

$$x_e \to 0 \quad \text{when} \quad t \to +\infty, \tag{35}$$

(c) if $\widehat{\mathcal{G}} = 0$ and $E_v \neq 0$, then x_e converges to zero when the time goes to infinity (i.e., (35) holds) and there exists a time instant $t_0^\star > t_0$ such that

$$\int_{t_0^\star}^{+\infty} \|x_e(t)\|^2 dt \leq \varepsilon_1 + \varepsilon_2 \int_{t_0^\star}^{+\infty} \|v(t)\|^2 dt, \tag{36}$$

where ε_1 and ε_2 are positive constants.

As for the minimal control synthesis (MCS) adaptive method,[31] Theorem 1 holds also for linear systems with time-varying parameters under the assumption that the adaptation rate of the integral part of the adaptive gains in (19a)–(19d) is faster than the rate of change of the system matrices in accordance with the following corollary.

Corollary 1. *Assuming time-varying matrices for the plant (2) whose rate of variation is such that*

$$\frac{d\widehat{\phi}}{dt} - \Gamma_\alpha w y_e^T \Gamma_N H \approx -\Gamma_\alpha w y_e^T \Gamma_N H, \tag{37}$$

where

$$w = \begin{bmatrix} x^T & r & d^T & y_I^T \end{bmatrix}^T \in \mathbb{R}^{n_w}, \tag{38}$$

then Theorem 1 still holds.

Remark.

- The matrix Γ_N is used for scaling the addends composing $H^T \Gamma_N y_e$ in (18), thus allowing it to weight each entries of y_e for the generation of the discontinuous control action. This could be useful for control problems where it is desirable that the discontinuous control action depends mainly on one output or a subset of outputs. The use of the Γ_N-matrix for the smart weighting of the output error components requires its inclusion in the adaptation laws (19a)–(19d) and in Assumption 3. The design of the feedback gain L for the reference model (3) based on the solution of an LMI, as required in Assumption 3, is common for output based MRAC strategies with closed-loop reference models (see for instance References 8 and 10 where the resulting LMIs are tailored for the proposed algorithm).
- The plant dynamics (2) is affected by two disturbances, *(i)* the disturbance d which could model measurable but non-manipulated plant inputs, and *(ii)* the disturbance $\mathcal{G}$ which represents unmodelled dynamics and unmeasurable external disturbances. For the disturbance $\mathcal{G}$, three components are considered as

its parametrization in (4), that is, *(i)* a matched bounded disturbance (i.e., $B_m g$); *(ii)* a non matched bounded disturbance (i.e., $\widehat{\mathcal{G}}$); and *(iii)* a square-measurable disturbance (i.e., $E_v v$). Theorem 1 assesses the closed-loop dynamics for different combinations of these three disturbance components.

- The knowledge of the sign of $\widehat{\phi}_R$ and conditions in Assumptions 1 and 2 are typical hypothesis for the design of MRAC strategies with gain locking methods.[30] However, nominal plant models are usually available for engineering control problems which can be exploited for designing of the reference model such that equalities (5) are satisfied. For instance the reference dynamics could be chosen as the closed-loop dynamics obtained by controlling the nominal plant model through linear control solutions (e.g., LQR methods as shown in Reference 2). Furthermore, knowledge of bounds for the plant parameters and disturbances is usually available for engineering problems and can be used, for example, for tuning the weights of the σ-modification strategies.[30]
- Similar to other output-based closed-loop MRAC solutions (i.e., Reference 8), the CL-EMRAC strategy requires knowledge of the output matrix C and the disturbance matrix E_v in the case that the plant dynamics are affected by an $\mathcal{L}_2$-disturbance. However, the knowledge of the matrix C is not as restrictive as it might appear at first. Indeed, for many control engineering problems, the matrix C is used for selecting the plant states that are measurable and available to controllers. Hence, the entries of the C-matrix are either zero or one in known positions. Furthermore, differently from other output-based closed-loop MRAC strategies, the CL-EMRAC algorithm can be implemented even if estimates of the E_v-matrix are not available or they are affected by high uncertainties. Indeed, if the E_v-matrix is unknown, the disturbance term $E_v v$ can be included in $\widehat{\mathcal{G}}$ and the ultimate boundedness of the closed-loop system can be proven.
- Compared to other output-based MRAC strategies with closed-loop reference model, for example, that presented in Reference 7, the CL-EMRAC algorithm not only augments the control action by adding the adaptive integral and adaptive switching control actions to improve robustness, that is, (14c) and (14d), respectively, but it also equips the adaptive control gains (19a)–(19d) with *(i)* a switching σ-modification strategy, which assures the ultimate boundedness of the closed-loop system and bounded adaptive gains in the presence of unmatched disturbances and unmodelled dynamics, without penalizing the adaptation of the control gains if their magnitude does not exceed a given threshold; and *(ii)* a proportional adaptive law as a faster adaptation mechanism for improving closed-loop tracking performance.[5] Moreover, the CL-EMRAC strategy provides an integral, a proportional and a leakage factor adaptive weight for each entry of the regressor (38), thus allowing tailoring of the contribution of each component of the w-regressor to the control action.
- The adaptive mechanism for the switching control adaptive gain, that is (19e), guarantees a bounded evolution of ϕ_N and its first derivative for any y_e-trajectory as $h_N(||y_e||_\Theta)$ in (20) is bounded for any y_e and the σ-modification strategy is used (see also Section 3.1).
- Conditions (9) and (10) can be replaced with a set of LMIs by using the approach presented in Reference 10. Indeed, $\theta > \theta^\star$ is satisfied when

$$\theta > \frac{\widehat{\phi}_{X,u}^2}{2\widehat{\phi}_{R,l}^2} \quad \Rightarrow \quad \frac{\widehat{\phi}_{X,u}^2}{2\widehat{\phi}_{R,l}^2} - \theta < 0, \tag{39}$$

and

$$\theta > \frac{\widehat{\phi}_{X,u}^2}{2\widehat{\phi}_{R,l}^2 \lambda_{\min}(Q)} \quad \Rightarrow \quad \frac{\widehat{\phi}_{X,u}^2}{2\widehat{\phi}_{R,l}^2} \mathcal{I}_{n_x} < \theta \lambda_{\min}(Q) \mathcal{I}_{n_x} < \theta Q \quad \Rightarrow \quad \frac{\widehat{\phi}_{X,u}^2}{2\widehat{\phi}_{R,l}^2} \mathcal{I}_{n_x} - \theta Q < 0. \tag{40}$$

Furthermore, condition (10) is equivalent to $\left\| PB_m - C^T \Gamma_N H \right\|^2 = 0$ which can be relaxed as

$$\left(PB_m - C^T \Gamma_N H\right)^T \left(PB_m - C^T \Gamma_N H\right) < \ell \quad \Rightarrow \quad \begin{bmatrix} \ell & \left(PB_m - C^T \Gamma_N H\right)^T \\ \star & -\mathcal{I}_{n_x} \end{bmatrix} < 0, \tag{41}$$

where the second inequality is obtained by the first one by using the Schur complement lemma with ℓ being a small positive constant.

Hence, Assumption 3 can be assessed by solving numerically the following optimization problem

$$\min \ell, \tag{42a}$$

$$\text{s.t. } (8), (39)\text{–}(41). \tag{42b}$$

This optimization problem is similar to that presented in Reference 10 with the additional constraint (39).

- The CL-EMRAC algorithm is more computationally demanding when compared to traditional MRAC and closed-loop MRAC solutions. Specifically, compared to the formers, the CL-EMRAC strategy requires for its design the solution of LMI (8)–(10) (or equivalently the optimization problem (42)) instead of the solution of a Lyapunov equation. Furthermore, compared to the traditional closed-loop MRAC strategy, the CL-EMRAC algorithm is more computationally demanding in terms of the computation of the control action as two additional adaptive control contributions must be computed. However, these increases of complexity are not as limitative as they might appear at first. Indeed, *(i)* nowadays there are efficient tools to solve LMIs problems (e.g., CVX[32]); and *(ii)* full-state feedback EMRAC solutions have been tested experimentally (see for instance Reference 1), thus suggesting that the increase of the computational effort caused by the addition of u_I and u_N does not prevent the real-time execution of controllers belonging to the EMRAC algorithms.

The design steps and the actions required for the computation of the CL-EMRAC control strategy are detailed in Algorithm 1, where T_f is the duration of the control task. Furthermore, for the procedure *CL-EMRAC_ACTION* it is assumed that the dynamic systems defining the evolution of the reference model (3) and the adaptive gains (19) have been discretized with a sampling time T_s.

Algorithm 1. CL-EMRAC strategy: design phase and operation for computing the control action

Design steps of the CL-EMRAC strategy.

Select the matrices A_m, E_m, B_m such that the matching conditions (5) hold;
Select the matrix Γ_N;
Compute P, Ω and H by solving the optimization problem (42);
Set $L := P^{-1}\Omega$;
Select the adaptive weights α_ι, β_ι, with $\iota \in \{X, R, D, I, N\}$, Θ and c_i, with $i = 1, 2, 3$, in (19) and (20), respectively;
Select the discharge factors ρ_ι, with $\iota \in \{X, R, D, I, N\}$ and the thresholds of the σ-modification strategy in (21);

Steps executed by the CL-EMRAC controller for the online computation of the control action.

procedure CL-EMRAC_ACTION
Set $t := 0$;
Select the initial state of the reference model (3);
Initialize the integral part of the adaptive gains, that is, ϕ_X, ϕ_R, ϕ_I, ϕ_D and ϕ_N;
while $t \leq T_f$ **do**
Read y, d and r;
Compute the output tracking error y_e by using (15);
Update the adaptive gains K_X, K_R, K_I, K_D and K_N by using (19);
Compute the control action u by using (13) and send it to the actuator system;
Update the state of the reference model x_m for the next iteration by using (3);
Compute the magnitude of ϕ defined in (22);
Compute the leakage factors f_X, f_R, f_I, f_D and f_N by using (21);
Update the integral part of the adaptive gains for the next iteration, that is, ϕ_X, ϕ_R, ϕ_I, ϕ_D and ϕ_N, by using (19);
$t := t + T_s$;
end while
end procedure

3 | PROOF OF THE MAIN THEOREM

The proof of Theorem 1 leverages on Lyapunov theory for smooth and non-smooth systems. The proof of Theorem 1 is structured as follow. In Section 3.1, the ultimate boundedness is proven for the adaptive control gain ϕ_N in (19e). It is noted that this is possible through the use of the novel adaptive mechanism, that is, the term $h_N(\|y_e\|_\Theta)$ in (20), which guarantees the boundedness of the derivative of ϕ_N for any evolution of y_e. Section 3.2 presents the derivation of closed-loop dynamics when the CL-EMRAC is used, the candidate Lyapunov function and its derivative along the closed-loop trajectories. Because the switching control action (14d) makes the closed-loop vector field discontinuous, differential inclusions are used to formulate the dynamics of the closed-loop control system. Finally, Sections 3.3 to 3.5 are dedicated to prove Theorem 1a to 1c, respectively. Corollary 1 is proven in Section 3.6.

The proof of Theorem 1 and the related remarks also require the following lemmas.

Lemma 1. *The σ-modification technique (21a) and (23) ensures that*

$$\frac{1}{\widehat{\phi}_R}\phi_e^T\Gamma_\alpha^{-1}f_\phi \geq 0,\ \forall\ \phi \in \mathbb{R}^{n_w}, \quad \text{and} \quad \frac{1}{\widehat{\phi}_R}\phi_e^T\Gamma_\alpha^{-1}f_\phi > 0,\ \forall\ \phi \in \mathbb{R}^{n_w}\ :\ \|\phi\| > \widehat{M}_\phi. \tag{43}$$

where

$$f_\phi = \begin{bmatrix} f_X^T & f_R & f_D^T & f_I^T \end{bmatrix}^T. \tag{44}$$

Furthermore,

$$\frac{1}{\widehat{\phi}_R}\phi_e^T\Gamma_\alpha^{-1}f_\phi > \frac{\eta_\phi}{2\widehat{\phi}_R}\phi_e^T\Gamma_\alpha^{-1}\Gamma_\rho\phi_e,\ \forall\ \phi \in \mathbb{R}^{n_w}\ :\ \|\phi\| > 2\widehat{M}_\phi. \tag{45}$$

Lemma 2. *For any compatible matrices $\mathcal{Z}$, $\mathcal{N}$ and $\mathcal{J}$, with $\mathcal{J}$ being a strictly positive matrix, the following matrix inequality is satisfied*

$$\mathcal{J}\mathcal{Z} + \mathcal{Z}^T\mathcal{J}^T \leq \varsigma^{-1}\mathcal{J}\mathcal{N}^{-1}\mathcal{J}^T + \varsigma\mathcal{Z}^T\mathcal{N}\mathcal{Z}, \tag{46}$$

where ς is a strictly positive constant.

Lemma 3. *Let Assumption 3 hold, then the matrix*

$$\widetilde{Q} = \begin{bmatrix} 2\theta C^T\Gamma_N HH^T\Gamma_N C & \frac{1}{\widehat{\phi}_R}C^T\Gamma_N H\widehat{\phi}_X^T \\ \frac{1}{\widehat{\phi}_R}\widehat{\phi}_X H^T\Gamma_N C & Q \end{bmatrix} \tag{47}$$

is positive definite.

Lemma 4. *Let Assumption 3 hold, then the matrix*

$$\Omega = -\left[P(A_m + LC) + (A_m + LC)^T P - \frac{2}{\widehat{\phi}_R}C^T\Gamma_N H\widehat{\phi}_X^T\right] \tag{48}$$

is strictly positive definite.

Lemma 5. *Given the discontinuous system*

$$\dot{\widetilde{x}} = \mathfrak{F}(t, \widetilde{x}), \tag{49}$$

with $\mathfrak{F} : \mathbb{R}^+ \times \mathbb{R}^n \to \mathbb{R}^n$ being a discontinuous vector field. If the differential inclusion

$$\dot{\widetilde{x}} \in \mathbf{K}[\mathfrak{F}]\left(t, \widetilde{x}\right) \quad (\text{with } \mathbf{K}[\mathfrak{F}] \text{ being the Filippov set valued map of } \mathfrak{F}) \tag{50}$$

is well-posed (i.e., for any initial condition a Filippov solution exists) and there exists a positive globally Lipschitz continuous function $V : \mathbb{R}^+ \times \mathbb{R}^n \to \mathbb{R}$, *two positive functions* $W_1, W_2 \in \mathcal{K}_\infty$, *a positive function* $W_3 \in \mathcal{K}$ *and a constant* $\mu > 0$ *such that*

$$W_1(\widetilde{x}) \leq V(t,\widetilde{x}) \leq W_2(\widetilde{x}), \quad \text{and} \quad \dot{\widetilde{V}}(t,\widetilde{x}) \leq -W_3(\widetilde{x}) \quad \forall \, \|\widetilde{x}\| \geq \mu, \tag{51}$$

where $\dot{\widetilde{V}}(t,\widetilde{x})$ *is the set-valued map defined in Reference* 33 as

$$\dot{\widetilde{V}} = \bigcap_{\xi \in \partial V(t,\widetilde{x})} \xi^{\mathrm{T}} \begin{pmatrix} \mathbf{K}[\mathcal{J}]\begin{pmatrix} t, \widetilde{x} \end{pmatrix} \\ 1 \end{pmatrix}, \text{ with } \partial V(t,\widetilde{x}) \text{ being the Clarke's generalised gradient.} \tag{52}$$

Then the non-smooth system (49) is globally uniformly ultimately bounded and the ultimate bound is given by $W_1^{-1}(W_2(\mu))$.

Lemma 1 can be proven as Lemma 2 in Reference 34, thus it is omitted for the sake of brevity. Lemma 2 is proven in Reference 35. The proof of Lemmas 3 and 4 are shown in Appendices A and B, respectively. Lemma 5 is a case of Theorem 3.1 presented in Reference 19 when *(i)* system (49) does not include time delays, *(ii)* the solution of the differential inclusion (50) exists for any initial condition, and *(iii)* the domain of $V(t,\widetilde{x})$ is $\mathbb{R}^+ \times \mathbb{R}^n$.

3.1 | Ultimate boundedness of the adaptive gain ϕ_N

The dynamics of ϕ_N in (19e) are smooth, thus the theory for nonlinear systems given in Reference 18 can be adopted to show that they are bounded and ultimate bounded.

Specifically, by selecting the functions V_N, W_{Na} and W_{Nb} as

$$V_N(\phi_N) = W_{Na}(\phi_N) = W_{Nb}(\phi_N) = \frac{\phi_N^2}{2}, \tag{53}$$

the following inequalities hold

$$W_{Na}(\phi_N) \leq V_N(\phi_N) \leq W_{Nb}(\phi_N). \tag{54}$$

As $h_N(\|y_e\|_\theta)$ is bounded for any evolution of y_e, it is possible to find a strictly positive constant c_N such that $h_N(\|y_e\|_\theta) \leq c_N$, $\forall \, y_e \in \mathbb{R}^{n_y}$. Hence, by using also the σ-modification strategy in (21b), after some algebraic manipulations, the derivative of $V_N(\phi_N)$ along the solutions of (19e) can be upper bounded as

$$\begin{aligned} \dot{V}_N &= \alpha_N h_N \phi_N - \sigma_N(\|\phi_N\|)\rho_N \phi_N^2 \\ &\leq -\rho_N \eta_N (1-\zeta_N)\phi_{Nj}^2 - \rho_N \eta_N \zeta_N \Phi_N^2 + \widetilde{c}_N \|\phi_N\| \\ &\leq -W_N(\phi_N), \quad \text{if} \quad \|\phi_N\| \geq \mu_N = \max\left\{ 2\widehat{M}_N, \frac{\widetilde{c}_N}{\rho_N \eta_N \zeta_N} \right\}, \end{aligned} \tag{55}$$

where $\widetilde{c}_N = |\alpha_N| c_N$, $\zeta_{Nj} \in (0,\ 1)$ and $W_N(\phi_N) = \rho_N \eta_N (1-\zeta_N)\phi_N^2$.

Now, as (55) holds, and the dynamics (19e) are smooth, Theorem 4.18, on page 172 in Reference 18, can be applied, which guarantees that the ϕ_N-dynamics are bounded and ultimate bounded, and the ultimate bound is $W_{Na}^{-1}(W_{Nb}(\mu_N)) = \mu_N$.

3.2 | Closed-loop dynamics

The closed-loop dynamics are obtained from (2), (3) and (13), and, after some algebraic manipulations, can be expressed as

$$\dot{x}_e = (A_m + LC)x_e + \frac{1}{\widehat{\phi}_R} B_m \left(\phi_e^T w - \widehat{\phi}_X^T x_e - \phi_N q_N(y_e) - H^T \Gamma_N y_e w^T \Gamma_\beta w \right) - \mathcal{G}, \tag{56a}$$

$$\dot{\phi}_e = -\Gamma_\alpha w y_e^T \Gamma_N H - f_\phi, \tag{56b}$$

where

$$f_\phi = -\sigma_\phi(\|\phi\|)\Gamma_\rho \phi_e, \tag{57}$$

$$\Gamma_\beta = \Delta(\beta_X, \beta_R, \beta_D, \beta_I) = \operatorname{diag}\left(\beta_1, \beta_2, \ldots, \beta_{n_w}\right) \in \mathbb{R}^{n_w \times n_w}, \tag{58}$$

with $\beta_j, j = 1, 2, \ldots, n_w$, being the jth entry on the diagonal of the matrix Γ_β.

The discontinuity of the term $q_N(y_e)$ makes the closed-loop dynamics (56) discontinuous, thus the theory presented in Reference 18 cannot be used to assess its ultimate boundedness. Hence, Filippov theory for non-smooth systems is used for studying the closed-loop dynamics (see also Appendix A in Reference 4 for the necessary background) and system (56) is substituted with the differential inclusion

$$\dot{\widetilde{x}}_e \in \mathbf{K}[\mathfrak{f}]\left(t, \widetilde{x}_e\right), \quad \text{and} \quad \widetilde{x}_e = \begin{bmatrix} x_e^T & \phi_e^T \end{bmatrix}^T, \tag{59}$$

where $\widetilde{x}_e$ is the stack of x_e and ϕ_e, while $\mathbf{K}[\mathfrak{f}]\left(t, \widetilde{x}_e\right)$ is the Filippov set valued map for the closed-loop discontinuous vector field obtained as

$$\begin{aligned} \mathbf{K}[\mathfrak{f}](t, \widetilde{x}_e) &= \mathbf{K}\begin{bmatrix} \left(A_m + LC\right) x_e + \frac{1}{\widehat{\phi}_R} B_m \left(\phi_e^T w - \widehat{\phi}_X^T x_e - \phi_N q_N(y_e) - H^T \Gamma_N y_e w^T \Gamma_\beta w \right) - \mathcal{G} \\ -\Gamma_\alpha w y_e^T \Gamma_N H - f_\phi \end{bmatrix} \\ &= \begin{bmatrix} \left(A_m + LC\right) x_e + \frac{1}{\widehat{\phi}_R} B_m \left(\phi_e^T w - \widehat{\phi}_X^T x_e - \phi_N \mathbf{K}\left[q_N(y_e)\right] - H^T \Gamma_N y_e w^T \Gamma_\beta w \right) - \mathcal{G} \\ -\Gamma_\alpha w y_e^T \Gamma_N H - f_\phi \end{bmatrix}, \end{aligned} \tag{60}$$

where the set valued map $\mathbf{K}\left[q_N(y_e)\right]$ is

$$\mathbf{K}\left[q_N(y_e)\right] = \mathbf{K}\left[\operatorname{sgn}(H^T \Gamma_N y_e)\right] = \begin{cases} -1, & \text{if } H^T \Gamma_N y_e < 0, \\ [-1, 1], & \text{if } H^T \Gamma_N y_e = 0, \\ 1, & \text{if } H^T \Gamma_N y_e > 0. \end{cases} \tag{61}$$

The following Lyapunov-like function is selected for the closed-loop dynamics (59),

$$V\left(\widetilde{x}_e\right) = \widetilde{x}_e^T \widetilde{P} \widetilde{x}_e, \tag{62}$$

where $\widetilde{P}$ is the strictly positive matrix defined in (31). The Lyapunov-like function (62) is lower bounded and upper bounded as

$$W_1\left(\widetilde{x}_e\right) \leq V\left(\widetilde{x}_e\right) \leq W_2\left(\widetilde{x}_e\right), \quad \text{with} \quad W_1\left(\widetilde{x}_e\right) = \lambda_{\min}(\widetilde{P})\left\|\widetilde{x}_e\right\|^2, \; W_2\left(\widetilde{x}_e\right) = \lambda_{\max}(\widetilde{P})\left\|\widetilde{x}_e\right\|^2, \tag{63}$$

where W_1 and W_2 are $\mathcal{K}_\infty$ functions.

As the function $V(\widetilde{x}_e)$ is smooth, its generalized derivative can be obtained in accordance with Reference 36 as $\dot{\tilde{V}} = \nabla V^T \mathbf{K}[\mathfrak{f}]$, which, after some algebraic manipulations, takes the following form

$$\begin{aligned}\dot{\tilde{V}} = x_e^T\left[P(A_m + LC) + (A_m + LC)^T P\right]x_e - \frac{2}{\widehat{\phi}_R} y_e^T \Gamma_N H \widehat{\phi}_X^T x_e - \frac{2}{\widehat{\phi}_R} y_e^T \Gamma_N H \phi_N \mathbf{K}\left[q_N(y_e)\right] \\ - \frac{2}{\widehat{\phi}_R} y_e^T \Gamma_N H H^T \Gamma_N y_e w^T \Gamma_\beta w - \frac{2}{\widehat{\phi}_R} x_e^T P \mathcal{G} - \frac{2}{\widehat{\phi}_R} \phi_e^T \Gamma_\alpha^{-1} f_\phi.\end{aligned} \tag{64}$$

Now, as the entries on the diagonal of Γ_β have the same sign of $\widehat{\phi}_R$, then the term $y_e^T \Gamma_N H H^T \Gamma_N y_e w^T \Gamma_\beta w / \widehat{\phi}_R$ is always positive, and consequently

$$\dot{\tilde{V}} \leq x_e^T\left[P(A_m + LC) + (A_m + LC)^T P\right]x_e - \frac{2}{\widehat{\phi}_R} y_e^T \Gamma_N H \widehat{\phi}_X^T x_e - \frac{2}{\widehat{\phi}_R} y_e^T \Gamma_N H \phi_N \mathbf{K}\left[q_N(y_e)\right] - 2x_e^T P \mathcal{G} - \frac{2}{\widehat{\phi}_R} \phi_e^T \Gamma_\alpha^{-1} f_\phi. \tag{65}$$

3.3 | Proof of Theorem 1a

To prove Theorem 1a, the target is to upper bound $\dot{\tilde{V}}$ with a strictly negative $\mathcal{K}$-function when the magnitude of $\widetilde{x}_e$ is sufficiently large, thus allowing the application of Lemma 5.

By using Assumption 3 and the Schur complement lemma to matrix Π in (8), the following matrix inequalities hold

$$\begin{aligned}P(A_m + LC) + (A_m + LC)^T P + Q + \mathcal{I}_{n_x} + 2\theta C^T \Gamma_N H H^T \Gamma_N C < 0 \Rightarrow \\ P(A_m + LC) + (A_m + LC)^T P < -Q - 2\theta C^T \Gamma_N H H^T \Gamma_N C - \mathcal{I}_{n_x},\end{aligned} \tag{66}$$

thus, $\dot{\tilde{V}}$ in (65) can be upper bounded as

$$\begin{aligned}\dot{\tilde{V}} &\leq -x_e^T \left[Q + \mathcal{I}_{n_x} + 2\theta C^T \Gamma_N H H^T \Gamma_N C + \frac{2}{\widehat{\phi}_R} C^T \Gamma_N H \widehat{\phi}_X^T\right] x_e - \frac{2}{\widehat{\phi}_R} y_e^T H \phi_N \mathbf{K}\left[q_N(y_e)\right] \\ &\quad - 2x_e^T P \mathcal{G} - \frac{2}{\widehat{\phi}_R} \phi_e^T \Gamma_\alpha^{-1} f_\phi \\ &= -x_e^T Q x_e - x_e^T x_e - 2\theta z_e^2 - \frac{2}{\widehat{\phi}_R} z_e \widehat{\phi}_X^T x_e - \frac{2}{\widehat{\phi}_R} y_e^T \Gamma_N H \phi_N \mathbf{K}\left[q_N(y_e)\right] - 2x_e^T P \mathcal{G} - \frac{2}{\widehat{\phi}_R} \phi_e^T \Gamma_\alpha^{-1} f_\phi,\end{aligned} \tag{67}$$

where

$$z_e = H^T \Gamma_N C x_e = x_e^T C^T \Gamma_N H \in \mathbb{R}. \tag{68}$$

Now, by complementing the square for the term $-2\theta z_e^2 - 2z_e \widehat{\phi}_X^T x_e / \widehat{\phi}_R$, inequality (67) can be further upper bounded as

$$\begin{aligned}\dot{\tilde{V}} &\leq -x_e^T Q x_e - \left(\sqrt{2\theta} z_e + \frac{1}{\widehat{\phi}_R \sqrt{2\theta}} \widehat{\phi}_X^T x_e\right)^2 + \frac{1}{2\theta \widehat{\phi}_R^2} x_e^T \widehat{\phi}_X \widehat{\phi}_X^T x_e - x_e^T x_e \\ &\quad - \frac{2}{\widehat{\phi}_R} y_e^T \Gamma_N H \phi_N \mathbf{K}\left[q_N(y_e)\right] - 2x_e^T P \mathcal{G} - \frac{2}{\widehat{\phi}_R} \phi_e^T \Gamma_\alpha^{-1} f_\phi \\ &\leq -x_e^T Q x_e + \frac{1}{2\theta \widehat{\phi}_R^2} x_e^T \widehat{\phi}_X \widehat{\phi}_X^T x_e - x_e^T x_e - \frac{2}{\widehat{\phi}_R} y_e^T \Gamma_N H \phi_N \mathbf{K}\left[q_N(y_e)\right] - 2x_e^T P \mathcal{G} - \frac{2}{\widehat{\phi}_R} \phi_e^T \Gamma_\alpha^{-1} f_\phi.\end{aligned} \tag{69}$$

According to (9), $\theta > \theta^\star \geq \widehat{\phi}_{X,u}^2 / (2\widehat{\phi}_{R,l}^2)$, thus

$$\frac{1}{2\theta \widehat{\phi}_R^2} x_e^T \widehat{\phi}_X \widehat{\phi}_X^T x_e - x_e^T x_e \leq \frac{1}{2\theta \widehat{\phi}_R^2} \left\|\widehat{\phi}_X\right\|^2 \|x_e\|^2 - \|x_e\|^2 < \left(\frac{\widehat{\phi}_{X,u}^2}{2\theta \widehat{\phi}_{R,l}^2} - 1\right) \|x_e\|^2 < 0, \tag{70}$$

and consequently,

$$\dot{\hat{V}} \leq -x_e^T Q x_e - \frac{2}{\hat{\phi}_R} y_e^T \Gamma_N H \phi_N \mathbf{K}\big[q_N(y_e)\big] - 2x_e^T P \mathcal{G} - \frac{2}{\hat{\phi}_R} \phi_e^T \Gamma_\alpha^{-1} f_\phi. \tag{71}$$

Now, starting from inequality (71), by completing the square and using (24) and (45), the generalized derivative $\dot{\hat{V}}$ can be further upper bounded as

$$\begin{aligned}
\dot{\hat{V}} &\leq -\frac{3}{4}\lambda_{\min}(Q)\|x_e\|^2 - \lambda_{\min}(Q)\left\|\frac{x_e}{2} + \frac{2P\mathcal{G}}{\lambda_{\min}(Q)}\right\|^2 + \frac{4\|P\mathcal{G}\|^2}{\lambda_{\min}(Q)} - \frac{2}{\hat{\phi}_R} y_e^T \Gamma_N H \phi_N \mathbf{K}\big[q_N(y_e)\big] - \frac{2}{\hat{\phi}_R}\phi_e^T \Gamma_\alpha^{-1} f_\phi \\
&\leq -\frac{3}{4}\lambda_{\min}(Q)\|x_e\|^2 + \frac{4\|P\|^2\|\mathcal{G}\|^2}{\lambda_{\min}(Q)} + \frac{3}{4}\lambda_{\min}(Q)\left(\left(2\widehat{M}_\phi + \|\widehat{\phi}\|\right)^2 - \|\phi_e\|^2\right) - \frac{2}{\hat{\phi}_R} y_e^T \Gamma_N H \phi_N \mathbf{K}\big[q_N(y_e)\big] \\
&\leq -\frac{3}{4}\lambda_{\min}(Q)\|\tilde{x}_e\|^2 + \frac{4\|P\|^2\mathcal{G}_\infty^2}{\lambda_{\min}(Q)} + \frac{3}{4}\lambda_{\min}(Q)\left(2\widehat{M}_\phi + \|\widehat{\phi}\|\right)^2 - \frac{2}{\hat{\phi}_R} y_e^T \Gamma_N H \phi_N \mathbf{K}\big[q_N(y_e)\big] \\
&= -\mu_1\|\tilde{x}_e\|^2 + \mu_2(\mathcal{G}_\infty) - \frac{2}{\hat{\phi}_R} y_e^T \Gamma_N H \phi_N \mathbf{K}\big[q_N(y_e)\big],
\end{aligned} \tag{72}$$

where $\mu_2(\widetilde{\mathcal{G}}_\infty)$ in (32) has been computed by setting $\widetilde{\mathcal{G}}_\infty^2 = \mathcal{G}_\infty^2$.

Moreover, if $g\widehat{\mathcal{G}}^T B_m \geq 0$, $\forall\ t \geq t_0$, by following the previous steps, it is possible to show that

$$\dot{\hat{V}} \leq -\mu_1\|\tilde{x}_e\|^2 + \mu_2(\widehat{\mathcal{G}}_\infty) - 2g y_e^T \Gamma_N H - \frac{2}{\hat{\phi}_R} y_e^T \Gamma_N H \phi_N \mathbf{K}\big[h_N(y_e)\big], \tag{73}$$

with $\mu_2(\widetilde{\mathcal{G}}_\infty^2)$ in (32) is obtained by setting $\widetilde{\mathcal{G}}_\infty^2 = \widehat{\mathcal{G}}_\infty^2 < \mathcal{G}_\infty^2$.

As

$$y_e^T \Gamma_N H \mathbf{K}\big[\mathrm{sgn}(H^T \Gamma_N y_e)\big] = \begin{cases} \big|y_e^T \Gamma_N H\big|, & \text{if} \quad y_e \neq 0, \\ 0, & \text{if} \quad y_e = 0,\ \forall\ \nu \in \mathbf{K}\big[\mathrm{sgn}(H^T \Gamma_N y_e)\big], \end{cases} \tag{74}$$

inequality (73) becomes

$$\dot{\hat{V}} \leq -\mu_1\|\tilde{x}_e\|^2 + \mu_2(\mathcal{G}_\infty) - \frac{2}{\hat{\phi}_R}\phi_N\big|y_e^T \Gamma_N H\big| \leq -\mu_1\|x_e\|^2 + \mu_2(\mathcal{G}_\infty). \tag{75}$$

Now, for any $\zeta \in (0,\ \ 1)$, inequality (75) can be further upper bounded as

$$\dot{\hat{V}} \leq -\mu_1\zeta\|\widetilde{x}_e\|^2 - \mu_1(1-\zeta)\|\widetilde{x}_e\|^2 + \mu_2(\mathcal{G}_\infty) \leq -W_3(\widetilde{x}_e), \quad \text{if} \quad \|\widetilde{x}_e\| \geq \sqrt{\frac{\mu_2(\mathcal{G}_\infty)}{\mu_1(1-\zeta)}} = \mu(\mathcal{G}_\infty), \tag{76}$$

with $W_3(\widetilde{x}_e) \in \mathcal{K}$ being the strictly positive function defined as

$$W_3(\widetilde{x}_e) = \mu_1\zeta\|\widetilde{x}_e\|^2. \tag{77}$$

As (63) and (76) hold, then the hypothesis of Lemma 5 are fulfilled, thus the trajectories of the closed-loop system (56)–(59) are uniformly ultimately bounded and the ultimate bound is $W_1^{-1}(W_2(\mu(\mathcal{G}_\infty))) = \sqrt{\frac{\lambda_{\max}(\widetilde{P})}{\lambda_{\min}(\widetilde{P})}}\mu(\mathcal{G}_\infty)$ as claimed in Theorem 1a when $\widetilde{\mathcal{G}}_\infty^2 = \mathcal{G}_\infty^2$. Furthermore, there exist a time interval $\mathcal{T}$, a $\mathcal{KL}$-class function $\Psi : \mathbb{R}^+ \times \mathbb{R}^+ \to \mathbb{R}^+$, and a

function $\gamma_b \in \mathcal{L}_\infty$ such that the dynamics of the closed-system are bounded as

$$\left\|\widetilde{x}_e(t)\right\| \leq \gamma_b(t), \quad \text{with} \quad \gamma_b(t) = \begin{cases} \Psi\left(\left\|\widetilde{x}_e(t_0)\right\|, t - t_0\right), & \text{if } t_0 \leq t < t_0 + \mathcal{T}, \\ \sqrt{\frac{\lambda_{\max}(\widetilde{P})}{\lambda_{\min}(\widetilde{P})}}\mu(\mathcal{G}_\infty), & \text{if } t > t_0 + \mathcal{T}. \end{cases} \tag{78}$$

In the case $g\widehat{\mathcal{G}}^T B_m \geq 0, \forall\, t \geq t_0$, from (74), the generalized derivative $\dot{\hat{V}}$ in (73) can be upper bounded as

$$\begin{aligned} \dot{\hat{V}} &\leq -\mu_1\left\|\widetilde{x}_e\right\|^2 + \mu_2\left(\widehat{\mathcal{G}}_\infty\right) - 2gy_e^T\Gamma_N H - \frac{2}{\widehat{\phi}_R}\phi_N\left|y_e^T\Gamma_N H\right| \\ &= -\mu_1\left\|\widetilde{x}_e\right\|^2 + \mu_2\left(\widehat{\mathcal{G}}_\infty\right) + 2g_\infty\left|y_e^T\Gamma_N H\right| - \frac{2}{\left|\widehat{\phi}_R\right|}|\phi_N|\left|y_e^T\Gamma_N H\right| \\ &\leq -\mu_1\left\|\widetilde{x}_e\right\|^2 + \mu_2\left(\widehat{\mathcal{G}}_\infty\right) - 2\left|y_e^T\Gamma_N H\right|\left[\frac{1}{\widehat{\phi}_{R,u}}|\phi_N| - g_\infty\right]. \end{aligned} \tag{79}$$

By considering the adaptation law (19e), there must exist a time instant $t_0^\star > t_0$ such that $|\phi_N| > g_\infty\widehat{\phi}_{R,u}, \forall\, t > t_0^\star$, thus (79) can be further upper bounded as

$$\dot{\hat{V}} \leq -\mu_1\zeta\left\|\widetilde{x}_e\right\|^2 + (1-\zeta)\mu_1\zeta\left\|x_e\right\|^2 + \mu_2\left(\widehat{\mathcal{G}}_\infty\right) \leq -W_3\left(\widetilde{x}_e\right), \quad \forall\, t \geq t_0^\star, \tag{80}$$

where $\zeta \in (0,\ 1)$ is a constant and $W_3\left(\widetilde{x}_e\right)$ is the strictly positive $\mathcal{K}$-function defined in (77).

Hence, assumptions for Lemma 5 are satisfied, and consequently the closed-loop system (56)–(59) is uniformly ultimately bounded with ultimate bound being $W_1^{-1}(W_2(\mu(\widehat{\mathcal{G}}_\infty))) = \sqrt{\frac{\lambda_{\max}(\widetilde{P})}{\lambda_{\min}(\widetilde{P})}}\mu(\widehat{\mathcal{G}}_\infty)$ as stated in Theorem 1a when $\widetilde{\mathcal{G}}_\infty^2 = \widehat{\mathcal{G}}_\infty^2$.

Furthermore, the closed-loop system dynamics can be upper bounded as

$$\left\|\widetilde{x}_e(t)\right\| \leq \gamma_b^\star(t), \quad \text{with} \quad \gamma_b^\star(t) = \begin{cases} \gamma_b(t), & \text{if } t_0 \leq t < t_0^\star, \\ \Psi^\star\left(||\widetilde{x}_e(t_0^\star)||, t - t_0^\star\right), & \text{if } t_0^\star \leq t < t_0 + \mathcal{T}^\star, \\ \sqrt{\frac{\lambda_{\max}(\widetilde{P})}{\lambda_{\min}(\widetilde{P})}}\mu(\mathcal{G}_\infty), & \text{if } t > t_0^\star + \mathcal{T}^\star, \end{cases} \tag{81}$$

where $\Psi^\star : \mathbb{R}^+ \times \mathbb{R}^+ \to \mathbb{R}^+$ is a $\mathcal{KL}$-class function and $\mathcal{T}^\star$ is a time interval that depends on the system initial conditions.

Now, (78) and (81) imply the boundedness of $\left\|\widetilde{x}_e\right\|$ and therefore the boundedness of x_e and ϕ_e. As x_e is bounded (i.e., $x_e \in \mathcal{L}_\infty$), then y_e is bounded while the boundedness of the integral of the output tracking error, that is, y_I, can be proven as in Reference 34. Inequality (66) implies that the matrix $A_m + LC$ is Hurwitz, thus the trajectory of the reference model is bounded. The boundedness of x_e and x_m implies that also x and y are bounded. Furthermore, as d, r, ϕ_e and x_e are bounded, then also K_X, K_R, K_I and K_D are limited. Finally, also u and $\dot{x}$ are bounded as the signals x, x_m, x_e, d, r, ϕ_N, K_X, K_R, K_I, and K_D are bounded. Hence, all the closed-loop signals are bounded, thus concluding the proof of Theorem 1a.

3.4 | Proof of Theorem 1b

In the case $\widehat{\mathcal{G}} = 0$ and $E_v = 0$, by using (43) and (74), after some algebraic manipulations, the generalized gradient (71) can be also upper bounded as

$$\begin{aligned} \dot{\hat{V}} &\leq -x_e^T Q x_e - 2gy_e^T\Gamma_N H - \frac{2}{\widehat{\phi}_R}\phi_N y_e^T\Gamma_N HK\left[\operatorname{sgn}(H^T\Gamma_N y_e)\right] \\ &\leq -\lambda_{\min}(Q)\|x_e\|^2 - 2\left|y_e^T\Gamma_N H\right|\left[\frac{1}{\widehat{\phi}_{R,u}}|\phi_N| - g_\infty\right] \leq -\lambda_{\min}(Q)\|x_e\|^2, \quad \forall\, t \geq t_0^\star, \end{aligned} \tag{82}$$

where $t_0^\star$ is the time instant after which $|\phi_N| \geq g_\infty\widehat{\phi}_{R,u}$ definitely.

In accordance with Theorem 2.2 in Reference 36, $\frac{dV}{dt}(\widetilde{x}_e(t),t) \in^{a.e} \dot{\tilde{V}}(\widetilde{x}_e(t),t)$, and therefore

$$\frac{dV}{dt}(\widetilde{x}_e(t),t) \leq^{a.e.} -\lambda_{\min}(Q)\|x_e\|^2, \quad \forall\, t \geq t_0^\star. \tag{83}$$

From inequality (83), the following integral inequality holds for any $t \geq t_0^\star$,

$$\int_{t_0^\star}^{t} \|x_e(\tau)\|^2 d\tau \leq \frac{1}{\lambda_{\min}(Q)}\left[V\left(\widetilde{x}_e(t_0^\star)\right) - V\left(\widetilde{x}_e(t)\right)\right] \leq \frac{V\left(\widetilde{x}_e(t_0^\star)\right)}{\lambda_{\min}(Q)} \tag{84}$$

along with any trajectory of the closed-loop system.

As (84) holds for $t \to +\infty$, then $x_e \in \mathcal{L}_2$. Moreover, the boundedness of all the closed-loop signals, proven in Section 3.3, implies $x_e \in \mathcal{L}_2 \cap \mathcal{L}_\infty$ and $\dot{x}_e \in \mathcal{L}_\infty$, thus

$$\frac{d}{dt}\left(\|x_e\|^2\right) = 2x_e^T\dot{x}_e \in \mathcal{L}_\infty. \tag{85}$$

Hence, Barbalat's lemma[30,37,38] can be used, and consequently $\|x_e(t)\|^2 \to 0$, which implies $x_e(t) \to 0$ when $t \to +\infty$.

3.5 | Proof of Theorem 1c

When $\widehat{\mathcal{G}} = 0$, by using (45) and (74), the generalized derivative in (65) can be upper bounded as

$$\dot{\tilde{V}} \leq x_e^T\left[P(A_m+LC)+(A_m+LC)^TP\right]x_e - \frac{2}{\widehat{\phi}_R}y_e^T\Gamma_N H\widehat{\phi}_X^T x_e - 2\left|y_e^T\Gamma_N H\right|\left[\frac{1}{\widehat{\phi}_{R,u}}|\phi_N| - g_\infty\right] - 2x_e^TPE_v v. \tag{86}$$

By using Assumption 3 and the Schur complement lemma to matrix (8), the following matrix inequalities hold

$$\begin{aligned} &P(A_m+LC)+(A_m+LC)^TP + \mathcal{I}_{n_x} + Q + 2\theta C^T\Gamma_N HH^T\Gamma_N C + \varepsilon^{-2}PE_vE_v^TP < 0 \Rightarrow \\ &P(A_m+LC)+(A_m+LC)^TP + \varepsilon^{-2}PE_vE_v^TP < -\mathcal{I}_{n_x} - Q - 2\theta C^T\Gamma_N HH^T\Gamma_N C. \end{aligned} \tag{87}$$

Furthermore, by setting $\varsigma = \varepsilon$, $\mathcal{J} = -x_ePE_v$, $\mathcal{Z} = v$ and $\mathcal{N} = \mathcal{I}_{n_v}$, the application of Lemma 2 allows to upper bound the term $-2x_e^TPE_vv$ as

$$-2x_e^TPE_vv = -x_e^TPE_vv - v^TE_v^TPx_e \leq \varepsilon^{-2}x_e^TPE_vE_v^TPx_e + \varepsilon^2v^Tv. \tag{88}$$

Hence, from (87) and (88), inequality (86) can be further upper bounded as

$$\begin{aligned} \dot{\tilde{V}} &\leq x_e^T\left[P(A_m+LC)+(A_m+LC)^TP\right]x_e - \frac{2}{\widehat{\phi}_R}y_e^T\Gamma_N H\widehat{\phi}_X^T x_e \\ &\quad - 2\left|y_e^T\Gamma_N H\right|\left[\frac{1}{\widehat{\phi}_{R,u}}|\phi_N| - g_\infty\right] + \varepsilon^{-2}x_e^TPE_vE_v^TPx_e + \varepsilon^2v^Tv \\ &< -x_e^T\left[\mathcal{I}_{n_x} + Q + 2\theta C^T\Gamma_N HH^T\Gamma_N C\right]x_e - \frac{2}{\widehat{\phi}_R}x_e^TC^T\Gamma_N H\widehat{\phi}_X^T x_e + \varepsilon^2v^Tv - 2\left|y_e^T\Gamma_N H\right|\left[\frac{1}{\widehat{\phi}_{R,u}}|\phi_N| - g_\infty\right] \\ &= -x_e^Tx_e + \varepsilon^2v^Tv - \widetilde{z}_e^T\widetilde{Q}\widetilde{z}_e - 2\left|y_e^T\Gamma_N H\right|\left[\frac{1}{\widehat{\phi}_{R,u}}|\phi_N| - g_\infty\right], \end{aligned} \tag{89}$$

where $\widetilde{z}_e = \begin{bmatrix} x_e^T & x_e^T \end{bmatrix}^T$ and $\widetilde{Q}$ is the matrix defined in (47).

In accordance with Lemma 3, $\widetilde{Q}$ is a positive matrix, thus the term $-\widetilde{z}_e^T\widetilde{Q}\widetilde{z}_e$ is negative. Moreover, for time instants $t \geq t_0^\star$, the last term in (89) is also negative, thus

$$\dot{\hat{V}} \leq -x_e^T x_e + \varepsilon^2 v^T v, \quad \text{when } t \geq t_0^\star. \tag{90}$$

Now, as $\frac{dV}{dt}(\widetilde{x}_e(t), t) \in^{a.e} \dot{\hat{V}}(\widetilde{x}_e(t), t)$, inequality (90) implies

$$\dot{V} \leq^{a.e.} -x_e^T x_e + \varepsilon^2 v^T v, \quad \text{when } t \geq t_0^\star, \tag{91}$$

By integrating inequality (91) and rearranging the resulting terms, the following integral inequality hold

$$V(\widetilde{x}_e(t)) - V(\widetilde{x}_e(t_0^\star)) + \int_{t_0^\star}^{t} \|x_e(\tau)\|^2 d\tau < \varepsilon^2 \int_{t_0^\star}^{t} \|v(\tau)\|^2 d\tau. \tag{92}$$

As $V(\widetilde{x}_e(t)) \geq 0$ for all time instants, when $t \to +\infty$ inequality (92) yields

$$\int_{t_0^\star}^{+\infty} \|x_e(\tau)\|^2 d\tau \leq V(\widetilde{x}_e(t_0^\star)) + \varepsilon^2 \int_{t_0^\star}^{+\infty} \|v(\tau)\|^2 d\tau, \tag{93}$$

which becomes (36) by setting $\varepsilon_1 = V(\widetilde{x}_e(t_0^\star))$ and $\varepsilon_2 = \varepsilon^2$.

The integral of inequality (91) also yields

$$V(\widetilde{x}_e(t)) + \int_{t_0^\star}^{t} \|x_e(\tau)\|^2 d\tau \leq V(\widetilde{x}_e(t_0^\star)) + \varepsilon^2 \int_{t_0^\star}^{t} \|v(\tau)\|^2 d\tau \leq V(\widetilde{x}_e(t_0^\star)) + \varepsilon^2 \mathcal{V}_2^2 < +\infty, \tag{94}$$

where $\mathcal{V}_2^2$ is the $\mathcal{L}_2$-norm of the disturbance v, which is supposed to be finite.

As (94) holds for any time instants and for $t \to +\infty$, then *(i)* $x_e \in \mathcal{L}_2$, and *(ii)* $V(\widetilde{x}_e(t))$ and $\widetilde{x}_e(t)$ are bounded for all time instants.

By using the same approach shown in Section 3.3, the boundedness of $\widetilde{x}_e(t)$ implies that all the closed-loop signals are bounded, thus $\dot{x}_e \in \mathcal{L}_\infty$, $x_e \in \mathcal{L}_2 \cap \mathcal{L}_\infty$ and $x_e^T \dot{x}_e \in \mathcal{L}_\infty$. Hence, the Barbalat's lemma can be applied as in Section 3.4, thus $x_e(t) \to 0$ when $t \to +\infty$, and consequently Theorem 1c remains proven and the proof of Theorem 1 is completed.

3.6 | Proof of Corollary 1

Corollary 1 extends the results shown in References 31 and 34 for MCS strategies to the CL-EMRAC algorithm.

Constant plant matrices in (2) imply that also the vector $\widehat{\phi}$ is constant, and consequently $\dot{\phi}_e = -\dot{\phi}$. Instead, for time varying matrices, the dynamics of ϕ_e are

$$\dot{\phi}_e = \dot{\widehat{\phi}} - \Gamma_\alpha w y_e^T \Gamma H - f_\phi.$$

However, the approximation in (37) yields

$$\dot{\phi}_e \approx -\Gamma_\alpha w y_e^T \Gamma H - f_\phi = -\dot{\phi}.$$

Hence, (56b) still holds, and thus Theorem 1 can be proven identically.

Remark.

- In the case of zero initial conditions and $\mathcal{G} = E_v v$ (i.e., $\widehat{\mathcal{G}} = 0$ and $g = 0$), then $t_0^\star = t_0$ and inequality (93) yields

$$\|x_e\|_{\mathcal{L}_2} \leq \varepsilon \|v\|_{\mathcal{L}_2}, \tag{95}$$

thus ε is the $\mathcal{L}_2$-gain of the closed-loop control system with respect to the disturbance v[18].

- The feedback gain L and the adaptive weights Γ_α make possible to decrease the state tracking error and its $\mathcal{L}_2$-norm in the case that the plant model is affected by matched disturbances (i.e., $\mathcal{G} = B_m g$). Indeed, under this condition, when $t \geq t_0^\star$ the generalized derivative in (86) can be upper bounded as

$$\dot{\widetilde{V}}(\widetilde{x}_e) \leq -x_e^T \Omega x_e \quad \Rightarrow \quad \dot{V}(\widetilde{x}_e) \leq^{a.e.} - \lambda_{\min}(\Omega)\|x_e\|^2, \tag{96}$$

where $\Omega = -\left[P(A_m + LC) + (A_m + LC)^T P - 2C^T \Gamma_N H \widehat{\phi}_X^T / \widehat{\phi}_R\right]$ is the strictly positive matrix in Lemma 4.

By integrating (96) and rearranging the terms, the following inequality hold

$$\begin{aligned} \int_{t_0^\star}^{+\infty} \|x_e(\tau)\|^2 d\tau &\leq \frac{V(\widetilde{x}_e(t_0^\star))}{\lambda_{\min}(\Omega)} = \frac{x_e^T(t_0^\star) P x_e(t_0^\star) + \phi_e^T(t_0^\star)\Gamma_\alpha^{-1}\phi_e(t_0^\star)/\widehat{\phi}_R}{\lambda_{\min}(\Omega)} \\ &\leq \frac{\lambda_{\max}(P)}{\lambda_{\min}(\Omega)}\left\|x_e(t_0^\star)\right\|^2 + \frac{1}{\lambda_{\min}(\Omega)\lambda_{\min}(\Gamma_\alpha/\widehat{\phi}_R)}\left\|\phi_e(t_0^\star)\right\|^2. \end{aligned} \tag{97}$$

Inequality (97) shows that by increasing the magnitude of the entries of the Γ_α-matrix, the second term for upper-bounding the $\mathcal{L}_2$-norm of the state tracking error reduces. Moreover, as $\lambda_{\min}(\Omega)$ depends on the feedback gain L, this gain gives a degree of freedom to adjust the first term of the upper bound for $\mathcal{L}_2$-norm which could not be modified otherwise. Consequently, the feedback gain L can help to further reduce the $\mathcal{L}_2$-norm, thus obtaining a better tracking of the reference trajectories which is also in-line with the results presented in Reference 8.

4 | APPLICATION OF THE OUTPUT-BASED CL-EMRAC STRATEGY TO DYC

This section describes an optimal method for the design of the reference dynamics for the output-based CL-EMRAC strategy to the DYC problem based a on simplified and linearized nominal vehicle model.

4.1 | Vehicle modeling

The vehicle model used for the DYC design is the dynamic bicycle model as it provides a good trade-off between accuracy and complexity[29] (see also Figure 2A for its schematic). Indeed, this model captures the key vehicle stability and characteristics during cornering despite its simplicity.

The vehicle states are the vehicle yaw rate, $\dot{\psi}$ and sideslip angle, β, whose dynamics are

$$m\left(v_x\dot{\beta} + v_x\dot{\psi}\right) = F_{yf} + F_{yr} \quad \text{and} \quad I_z\ddot{\psi} = L_a F_{yf} - L_b F_{yr} + u, \tag{98}$$

where v_x is the longitudinal speed, m is the vehicle mass, I_z is the yaw mass moment of inertia, L_a and L_b are the front and rear semi-wheelbases, F_{yf} and F_{yr} are the front and rear lateral tire forces, respectively, and u is the direct yaw moment, that is, the control action generated by DYC strategies and actuated by low level controllers.

The lateral tire forces depend on the wheel slip angles and are highly nonlinear and their modeling is usually affected by large uncertainties, thus making the robust tracking of reference dynamics a challenging task. However, for the control design, linear approximations of the tire models are usually adopted, thus the resulting vehicle dynamics are linear and described by model (2). Specifically, in accordance to Reference 29, by selecting as system state $x = \begin{bmatrix}\beta & \dot{\psi}\end{bmatrix}^T$, the system

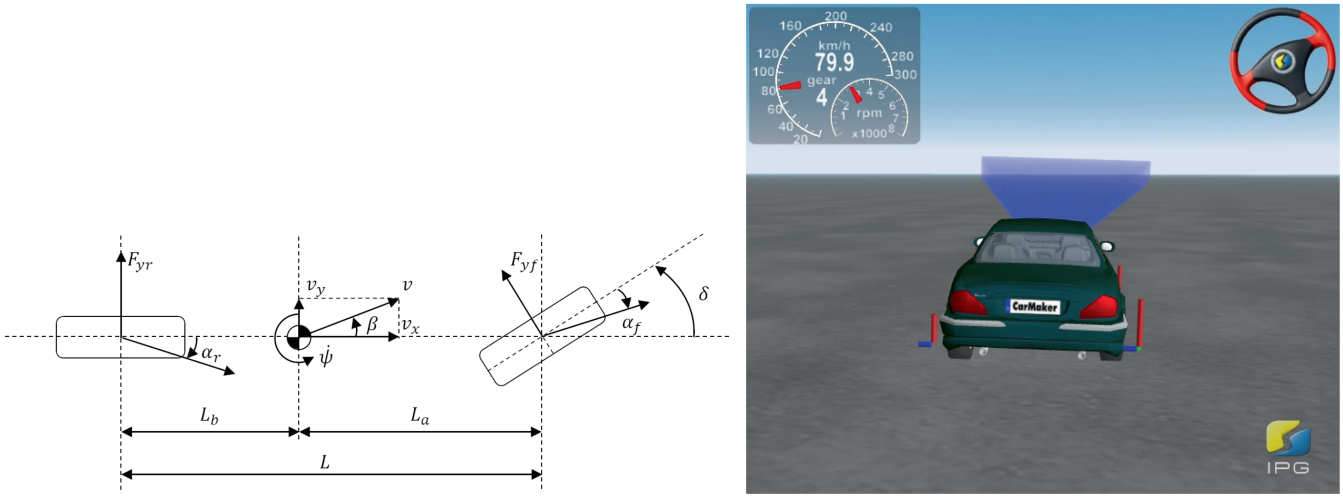

FIGURE 2 (A) Schematic of the bicycle model, where v_y is the lateral speed, and α_f and α_r are the front and rear slip angles, respectively; and (B) view of the IPG CarMaker vehicle model in the testing environment.

matrices and disturbances for the plant model are

$$A = \begin{bmatrix} -\frac{C_{\alpha f}+C_{\alpha r}}{mv_x} & \frac{C_{\alpha r}L_b - C_{\alpha f}L_a}{mv_x^2} - 1 \\ \frac{C_{\alpha r}L_b - C_{\alpha f}L_a}{I_z} & -\frac{C_{\alpha r}L_b^2 + C_{\alpha f}L_a^2}{I_z v_x} \end{bmatrix}, \quad B = \begin{bmatrix} 0 \\ \frac{1}{I_z} \end{bmatrix}, \quad E = \begin{bmatrix} \frac{C_{\alpha f}}{mv_x} \\ 0 \end{bmatrix}, \quad C = \begin{bmatrix} 0 & 1 \end{bmatrix}, \tag{99}$$

$$E_v = 0, \quad g = \frac{L_a C_{\alpha f}}{b_{m2} I_z}\delta, \quad d = \delta, \tag{100}$$

where $C_{\alpha f}$ and $C_{\alpha r}$ are the front and rear cornering stiffness, respectively, δ is the front steering angle and b_{m2} is the second component of the reference model used to describe the effect of the steering angle on the yaw rate dynamics as a matched disturbance of the form $B_m g$. The unmatched disturbance $\widehat{\mathcal{G}}$ in (4) can model mismatches due to tire modeling uncertainties and linear approximation; plant parameter variations, for example, vehicle speed around the nominal condition; and external disturbances.

It is noted that, according to the matrix C in (99), the only state available to the controller is the yaw rate, thus costly sensor and/or state estimators for the sideslip angle can be avoided.

4.2 | Selection of the reference dynamics

Based on the nominal plant parameters, the reference dynamics are selected as the closed-loop dynamics obtained when the nominal vehicle model is controlled via an LQR strategy. Specifically, this article extends the LQ design of the reference model presented in Reference 2 by using the LQR formulation in the presence of measurable disturbances.[39] Hence, the reference dynamics are designed by solving the following LQR problem

$$\min_{u(\cdot)} \int_{t_0}^{+\infty} (r - Cx)^T Q_0 (r - Cx) + R_0 u^2 d\tau, \tag{101a}$$

$$\text{s.t.} \quad \dot{x} = A_0 x + B_0 u + E_0 d, \tag{101b}$$

where A_0, B_0, and E_0 are the nominal values for the system matrices in (99), Q_0 and R_0 are strictly positive weights of the cost function, and $r = \dot{\psi}_r$ is the reference yaw rate.

The optimal control problem in (101) is solved with a linear control strategy of the form $u_{\text{opt}} = K_X^\star x + K_R^\star r + K_D^\star d$, with $K_X^\star$, $K_R^\star$ and $K_D^\star$ being the optimal control gains. Hence, the matrices of the reference model (3) are set as

$$B_m = B_0 K_R^\star, \quad A_m = A_0 + B_0 K_X^\star, \quad E_m = E_0 + B_0 K_D^\star. \tag{102}$$

The reference input $r = \dot{\psi}_r$ depends on the steering angle and is selected as in Reference 29

$$\dot{\psi}_r = \min\left\{|r_{ss}|, c\frac{\mu_r g_a}{v_x}\right\}\text{sgn}(\delta), \quad \text{and} \quad r_{ss} = \frac{v_x}{(L_a + L_b)(1 + k_{us} v_x^2)}\delta, \tag{103}$$

where μ_r is the road friction coefficient, c is a safety factor and k_{us} is the understeer gradient.

5 | NUMERICAL RESULTS

The effectiveness of the CL-EMRAC strategy to impose the desire vehicle dynamics has been tested in a co-simulation environment based on IPG CarMaker and MATLAB/Simulink. IPG CarMaker simulates the vehicle dynamics, through detailed non-linear models, for example, a nonlinear tire model, thus providing a reliable simulation environment for assessing vehicle control functionalities, while the controllers are implemented in Simulink. The main vehicle parameters are listed in Table 1, and Figure 2B shows the vehicle in the simulation environment.

The cornering stiffness coefficients in Table 1 have been obtained by linearizing the nonlinear tire characteristics at the origin for control design purposes only. For this case study, the disturbance $\mathcal{G}$ is the mismatch between the bicycle model in Section 4.1 and the nonlinear IPG CarMaker model.

The reference model (3) has been selected as detailed in Section 4.2, for $v_x = 80$ km/h. Moreover, for the design of the reference model matrices *(i)* a mismatch of approximately 15% has been assumed in the vehicle parameters, that is, $C_{\alpha f}$, $C_{\alpha r}$, m and I_z, with respect to their actual values in Table 1; *(ii)* the cost weights Q_0 and R_0 have been tuned to have a good tracking of the reference yaw rate; and *(iii)* the feedback gain L has been computed numerically by using CVX.[40]

For the implementation of the CL-EMRAC strategy, the adaptive weights have been chosen as a trade-off between convergence time and reactivity of the control action, and the sign function has been smoothed as in Reference 2 to avoid chattering.

The steering input δ is set as the concatenation of the following sub-maneuvers: *(i)* a sinusoidal wave with 270 deg amplitude and 0.25 Hz frequency for $t \in [0, \ 10]$ s; *(ii)* a sinusoidal wave with 270 deg amplitude and 1 Hz frequency for $t \in [15, \ 20]$ s; *(iii)* a ramp steer ranging from 0 deg to 150 deg with a rate of change 10 deg/s for $t \in [25, \ 45]$ s; *(iv)* the sine-with-dwell (SWD) maneuver defined in the FMVSS126 standard for electronic stability control (ESC) systems,[41] with 270 deg amplitude for $t \in [50, \ 52]$ s; and *(v)* a double step steer with 100 deg steering amplitude, occurring with positive and negative steering inputs at $t = 60$ s and $t = 65$ s, respectively. Outside the aforementioned time ranges, the steering angle is set to zero.

TABLE 1 Main vehicle parameters.

Parameter	Value	Description
L_a	1.41 m	Front semi-wheelbase
L_b	1.23 m	Rear semi-wheelbase
$C_{\alpha f}$	1.11×10^5 N/rad	Front axle cornering stiffness
$C_{\alpha r}$	1.18×10^5 N/rad	Rear axle cornering stiffness
I_z	2469 kg m^2	Vehicle moment of inertia
m	1534 kg	Vehicle mass
K_{us}	1.87×10^{-4} (kg/m) (rad/N)	Vehicle stability factor
μ_r	0.85	Friction coefficient
SR	0.046	Steering ratio

5.1 | Closed-loop behavior

In this section the closed-loop dynamics obtained when the IPG CarMaker model is controlled by the output-based CL-EMRAC strategy are presented.

Figure 3 depicts the closed-loop tracking error, and shows that the yaw rate error never exceeds 0.1 rad/s, while the sideslip angle error is below 1.8 deg for the entire maneuver. The zooms in Figure 3A,B show that the rapid variation of the error occurs in the time interval [15, 20] s, and is caused by the swift (at 1 Hz) variation of the driver input.

The small tracking error results in a very good tracking of the reference model over the entire maneuver, as confirmed in Figure 4. In addition to the reference model and plant trajectory for each sub-maneuver, Figure 4 also shows the dynamics of the passive vehicle (i.e., without control). For the passive vehicle, at the end of the second sub-maneuver (i.e., the sinusoidal steering wave at 1 Hz) the magnitude of the sideslip angle exceeds 15 deg (see also Figure 4F) and the vehicle rolls over, thus the simulation stops. The inability of the passive vehicle to complete the maneuver confirms the need for effective stability control. In this framework, the CL-EMRAC strategy is a viable solution, as it allows to precisely track the reference dynamics also during rapid and severe variations of the steering input, for example, the sine-with-dwell maneuver in Figure 4D,H.

The dynamics of the norm of the integral part of the adaptive gains, that is, the norm of ϕ_N in (19e) and ϕ in (22), are depicted in Figure 5, along with the thresholds for the activation of the corresponding σ-modification strategy. Figure 5A shows that $\|\phi\|$ exceeds the threshold $2\widehat{\mathcal{M}}_\phi$ during the sinusoidal maneuver at 1 Hz and the sine-with-dwell test. Hence, these two sub-maneuvers require the use of the largest leakage factor to prevent control gains drift, thus these maneuvers are the most challenging among the selected ones. After the completion of the sine-with-dwell (i.e., $t > 52$ s), the norm of the integral part of the adaptive gains, that is, $\|\phi\|$, stays below $\widehat{\mathcal{M}}_\phi$, and thus the σ-modification remains inactive. Figure 5B shows that ϕ_N is bounded and within $\left[\widehat{\mathcal{M}}_{\phi_N},\ 2\widehat{\mathcal{M}}_{\phi_N}\right]$ for $t > 10$ s, thus implying the activation of the σ-modification σ_N in (28) in this time range. As the term h_N in (20) is strictly positive, the dynamics of $\|\phi_N\|$ are strictly increasing for $t < 10$ s, and without the use of σ_N they would keep unboundedly increasing, and eventually lead to closed-loop instability. The boundedness of the norm of the integral part of the adaptive gains and the boundedness of the tracking error (see also Figure 3) imply the boundedness of the adaptive gains and control action in (19a)–(19d) and (13), respectively.

5.2 | Tracking performance comparison via KPIs

The tracking performance of the output-based CL-EMRAC strategy is compared to those provided by four benchmark controllers. Specifically, the following control solutions have been designed and implemented

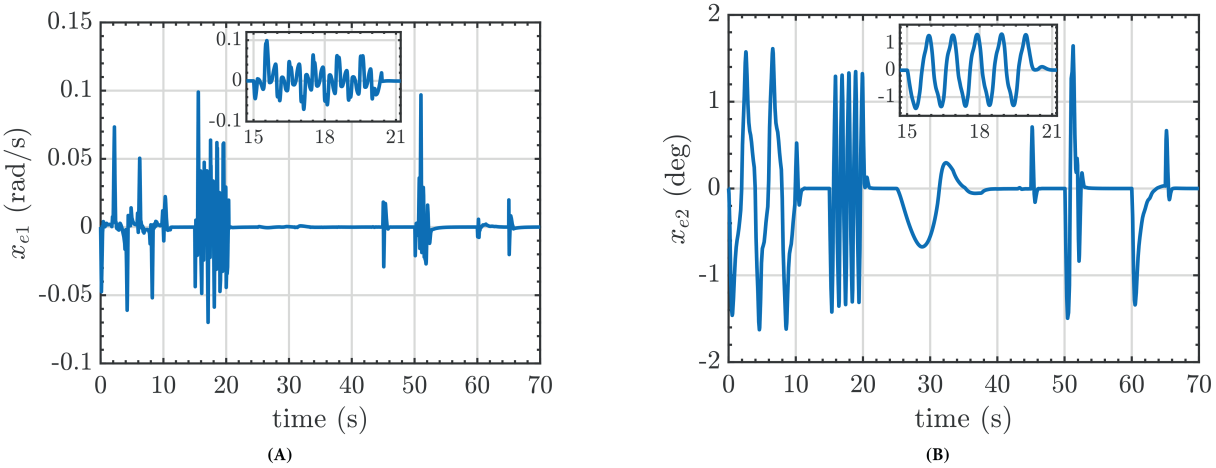

FIGURE 3 Error dynamics with the output-based CL-EMRAC strategy: (A) yaw rate error and (B) sideslip angle error.

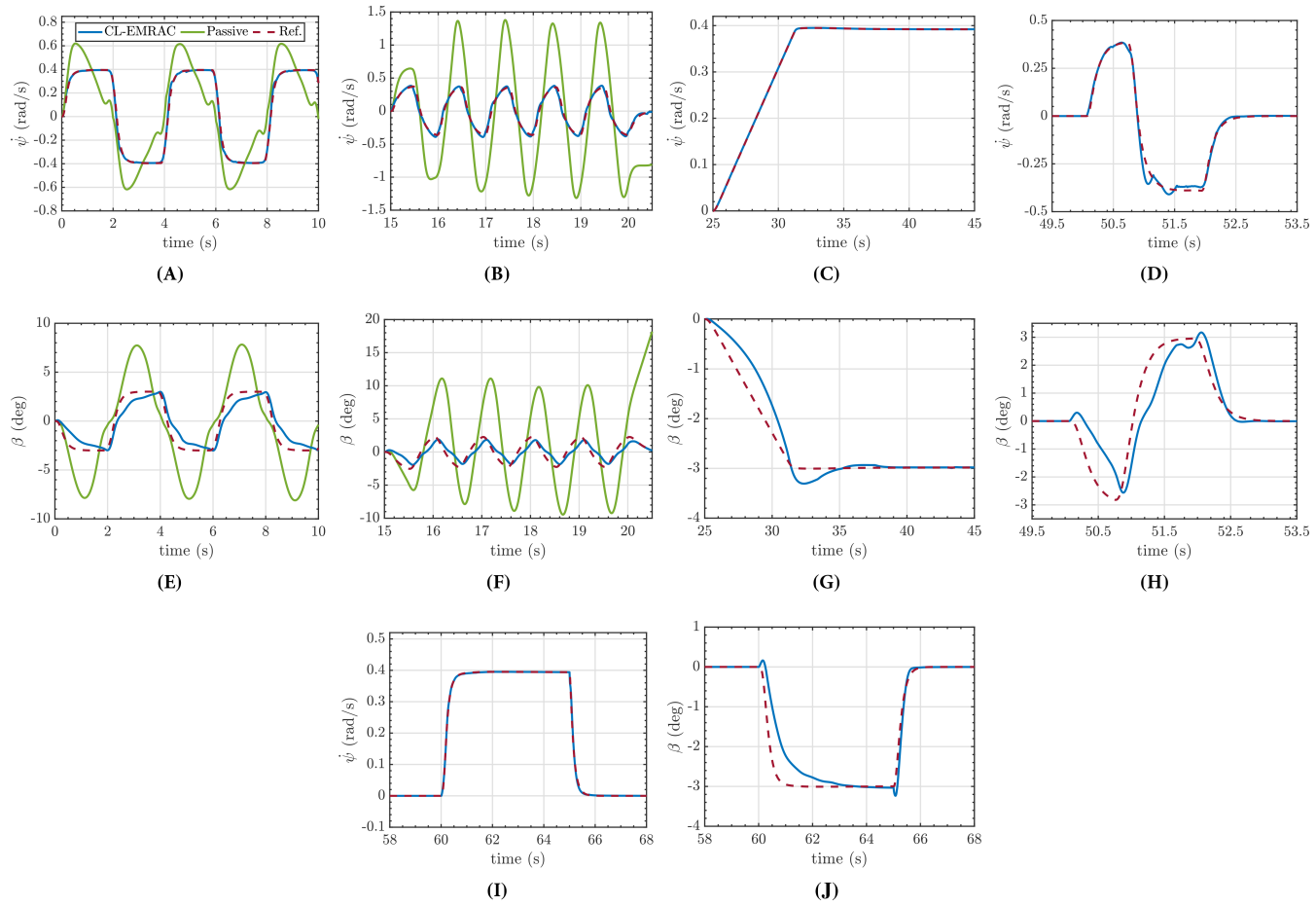

FIGURE 4 Tracking performance for each sub-maneuver. Reference model (red dashed line), the passive vehicle (green solid line) and output-based CL-EMRAC algorithm (blue solid line). Sinusoidal steering at 0.25 Hz (A, E); sinusoidal steering at 1 Hz (B, F); ramp steer (C, G); sine-with-dwell maneuver (D, H); and step steer (I, J).

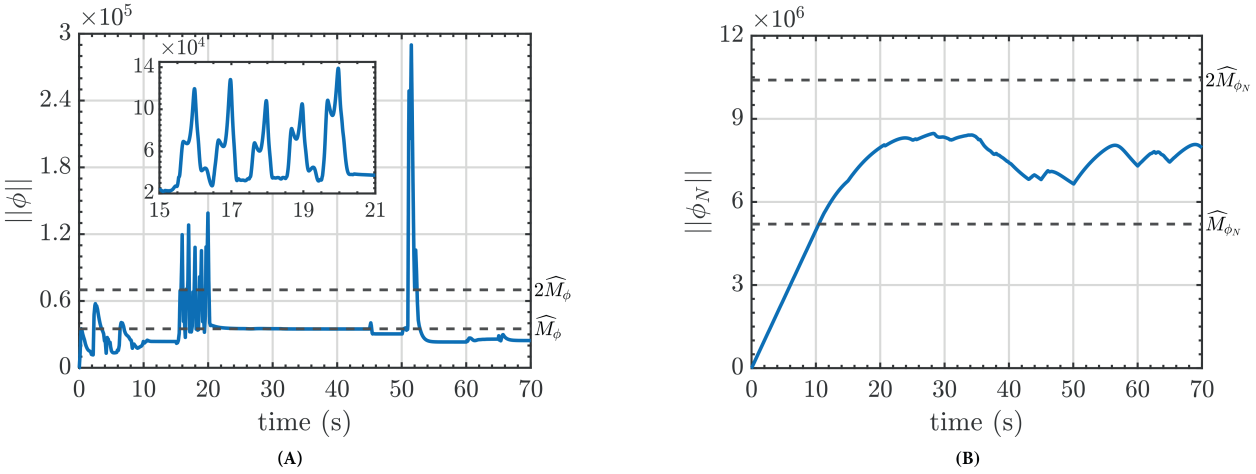

FIGURE 5 Norm of the integral part of the output-based CL-EMRAC adaptive gains (A) $\|\phi\|$ and (B) $\|\phi_N\|$.

- *LQR*. The linear-quadric regulator (LQR) approach presented in Reference 29 is a full-state feedback optimal strategy to steer the dynamics of the yaw rate towards the required reference. The control strategy consists of a model-based feed-forward action augmented with a gain scheduling feedback LQ control action. The reference yaw rate and sideslip angle provided to the LQ controller are the reference states generated by the model in Section 4.2, that is, the linear system with matrices (A_m, B_m, E_m) in (102). This LQ algorithm has been selected as a benchmark controller as LQ strategies are commonly used for solving the direct yaw moment control problem.[42]
- *RLQR*. According to Reference 42 LQR solutions are very sensitive to vehicle mismodelling and perturbations, thus requiring adjustments for making the closed-loop tracking performance robust. Hence, also the robust LQR (RLQR) strategy in Reference 29 has been implemented. In the RLQR, the closed-loop robustness to model mismatches and disturbances is obtained by augmenting the LQR algorithm with an additional gain scheduling full-state feedback action based on the state tracking error.
- *MRAC*. This control strategy is the classical full-state model reference adaptive control with integral adaptive control gains presented, for instance, in Reference 30. The reference model has been selected in accordance with the approach presented in Section 4.2, see (A_m, B_m, E_m) in (102). The adaptive weights have been tuned as a trade-off between tracking performance and reactivity of the control action.
- *CL-MRAC*. This control solution is the output-based closed-loop model reference adaptive control strategy obtained by excluding the adaptive switching control action and the integral adaptive action from the output-based CL-EMRAC. Consequently, the reference model and the adaptive weights are the same of the CL-EMRAC solution, but the control action (13) is computed by setting $u_I = u_N = 0$. The CL-MRAC is used to show the improvement of the tracking performance obtained through the use of the integral and switching control actions.

For the design of the LQR strategies and the reference model for the benchmark adaptive solutions, a parameter uncertainty of approximately 15% has been assumed.

The error dynamics for each benchmark controller are reported in Figure 6. When compared to Figure 6, Figure 3 shows that the output based CL-EMRAC algorithm provides better tracking performance. However, for a quantitative comparison, the control solutions are evaluated for each sub-maneuver through the use of a set of key performance indicators (KPIs), that is: *(i)* the root mean square error of the yaw rate ($\text{RMSE}_{\dot{\psi}}$); *(ii)* the root mean square error of the sideslip angle (RMSE_{β}); *(iii)* the maximum error of the yaw rate ($\text{ME}_{\dot{\psi}}$); *(iv)* the maximum error of the sideslip angle (ME_{β}); and *(v)* the integral of absolute value of control action (IACA). The first four KPIs evaluate the tracking performance of the closed-loop control system while the IACA is a measurement of the control effort.

Table 2 reports the KPIs computed for each sub-maneuver and for each control strategy, based on which the following remarks are made.

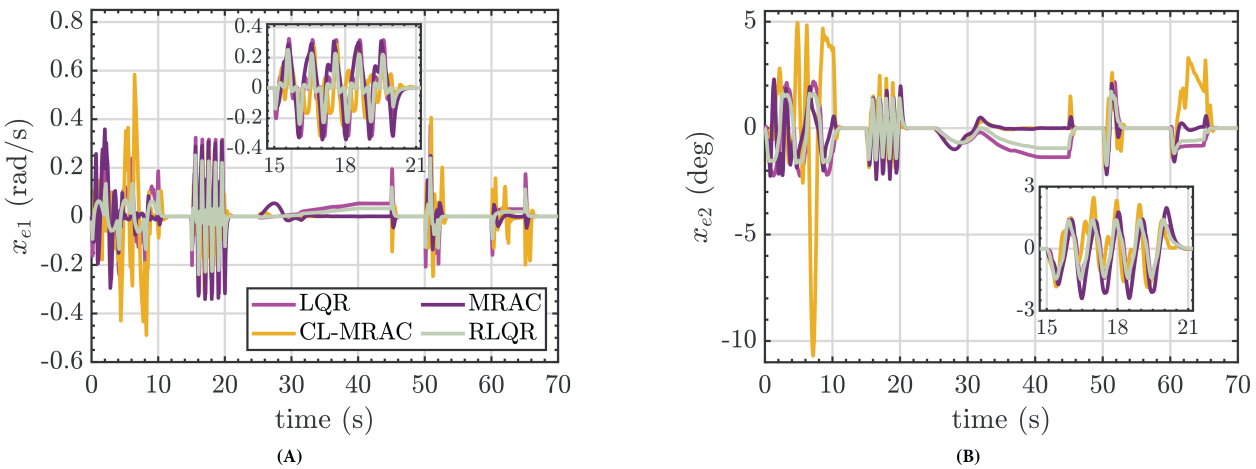

FIGURE 6 Error dynamics when the benchmark control solutions are used: (A) yaw rate error and (B) sideslip angle error.

TABLE 2 KPIs for each control solution.

Sub-maneuvers	KPI	CL-EMRAC	CL-MRAC	MRAC	RLQR	LQR
Sinusoidal 0.25 Hz	$RMSE_{\dot{\psi}}$ (rad/s)	1.53E−02	2.00E−01	1.14E−01	5.80E−02	1.04E−01
	$RMSE_{\beta}$ (deg)	8.81E−01	3.58E+00	1.17E+00	1.29E+00	1.63E+00
	$ME_{\dot{\psi}}$ (rad/s)	7.55E−02	5.78E−01	3.58E−01	1.35E−01	2.40E−01
	ME_{β} (deg)	1.62E+00	1.06E+01	2.29E+00	1.63E+00	2.22E+00
	IACA (Nm)	2.99E+03	1.07E+04	5.40E+03	3.67E+03	5.00E+03
Sinusoidal 1 Hz	$RMSE_{\dot{\psi}}$ (rad/s)	3.26E−02	1.29E−01	1.84E−01	1.09E−01	1.51E−01
	$RMSE_{\beta}$ (deg)	9.05E−01	1.12E+00	1.26E+00	9.25E−01	9.25E−01
	$ME_{\dot{\psi}}$ (rad/s)	1.03E−01	3.09E−01	3.41E−01	2.53E−01	3.26E−01
	ME_{β} (deg)	1.42E+00	2.41E+00	2.40E+00	1.50E+00	1.71E+00
	IACA (Nm)	9.74E+03	1.09E+04	1.06E+04	9.12E+03	9.01E+03
Ramp steer	$RMSE_{\dot{\psi}}$ (rad/s)	2.01E−04	3.39E−03	1.68E−02	2.16E−02	3.56E−02
	$RMSE_{\beta}$ (deg)	2.80E−01	2.83E−01	3.60E−01	6.70E−01	9.51E−01
	$ME_{\dot{\psi}}$ (rad/s)	7.15E−04	1.51E−02	5.39E−02	3.32E−02	5.34E−02
	ME_{β} (deg)	6.72E−01	6.70E−01	9.99E−01	9.45E−01	1.36E+00
	IACA (Nm)	1.93E+02	2.60E+02	4.63E+02	5.84E+02	1.68E+03
Sine-with-dwell	$RMSE_{\dot{\psi}}$ (rad/s)	2.81E−02	1.40E−01	9.86E−02	6.97E−02	1.20E−01
	$RMSE_{\beta}$ (deg)	1.03E+00	1.25E+00	1.35E+00	1.27E+00	1.34E+00
	$ME_{\dot{\psi}}$ (rad/s)	9.84E−02	4.12E−01	2.49E−01	2.40E−01	3.74E−01
	ME_{β} (deg)	1.64E+00	2.55E+00	2.18E+00	1.75E+00	2.16E+00
	IACA (Nm)	8.33E+03	1.13E+04	5.52E+03	7.28E+03	8.83E+03
Step steer	$RMSE_{\dot{\psi}}$ (rad/s)	2.35E−03	4.90E−02	1.58E−02	1.98E−02	3.33E−02
	$RMSE_{\beta}$ (deg)	3.60E−01	1.50E+00	3.65E−01	4.75E−01	5.96E−01
	$ME_{\dot{\psi}}$ (rad/s)	2.11E−02	1.96E−01	6.36E−02	1.11E−01	1.74E−01
	ME_{β} (deg)	1.34E+00	3.32E+00	1.58E+00	1.19E+00	1.06E+00
	IACA (Nm)	5.47E+02	3.53E+03	5.63E+02	9.17E+02	1.59E+03

- The CL-EMRAC algorithm outperforms the LQ solutions, as it brings a reduction of the tracking performance indicators for several sub-maneuvers. For instance, $RMSE_{\dot{\psi}}$ substantially reduces for all the sub-maneuvers when compared to the LQR and RLQR solutions. $RMSE_{\beta}$ is similar to that provided by the LQ strategies only for the sinusoidal steering section at 1 Hz. However, for the remaining sub-maneuvers, $RMSE_{\beta}$ improves by at least 20%. Hence, the CL-EMRAC strategy is an effective alternative to full-state feedback LQ control strategies, for increasing robustness to parameter uncertainties and unmodelled nonlinear dynamics.
- All the tracking performance indicators improve when the CL-EMRAC strategy replaces the classical MRAC algorithm, with a notable reduction of $RMSE_{\dot{\psi}}$ and $ME_{\dot{\psi}}$. Furthermore, $ME_{\dot{\beta}}$ improves by at least 15%, while the $RMSE_{\beta}$ value of the CL-EMRAC solution is comparable to that obtained via the MRAC algorithm only for the step steer maneuver, while reductions of this KPI are observed for the other sub-maneuvers. The output-based CL-EMRAC outperforms the standard MRAC algorithm not only because it is enhanced with robust adaptive control actions, but also because the σ-modification strategy prevents the drift of the adaptive gains due to the unmatched disturbances, and the addition of the proportional part to the adaptive laws quickly adjusts the control gains in presence of rapid variations of the tracking error.
- Among the benchmark control solutions, the output-based CL-MRAC is the least capable of imposing the reference dynamics for most of the sub-maneuvers. Indeed, all the tracking KPIs of the CL-MRAC are better than those obtained by the remaining benchmark controllers only in the case of the ramp steer maneuver. For the other sub-maneuvers,

worse or comparable performance is generally obtained. For instance, all the KPIs provided by the CL-MRAC are the worst when considering the sinusoidal steering section at 0.25 Hz and the step steer. Similarly, $\text{RMSE}_{\dot{\psi}}$, $\text{ME}_{\dot{\psi}}$ and ME_{β} for the SWD maneuver and RMSE_{β} for the sinusoidal steering maneuver at 1 Hz are the highest for the CL-MRAC. This result shows that the CL-MRAC strategy is not robust with respect to persistent unmodelled mismatches and disturbances. In this framework, the novel CL-EMRAC algorithm represents a possible approach to improve the tracking performance of the CL-MRAC algorithm for $\mathcal{L}_\infty$ unknown nonlinear dynamics and disturbances.

- The KPIs obtained with the CL-EMRAC solutions are smaller than those provided by the CL-MRAC. Specifically, for each sub-maneuver, $\text{RMSE}_{\dot{\psi}}$ and $\text{ME}_{\dot{\psi}}$ reduce in excess of 65%. The sideslip angle tracking performance provided by the CL-EMRAC is comparable to that of the CL-MRAC only for the ramp steer maneuver. For the other sub-maneuvers, RMSE_{β} decreases by at least 17.5%, while $\text{ME}_{\dot{\psi}}$ by more than 35%. Consequently, Table 2 highlights the substantial improvement provided by the adaptive switching and adaptive integral control actions included in the CL-EMRAC. These additional control actions enhance the baseline CL-MRAC strategy, and enable it to tackle the unmatched unmodelled dynamics, thus outperforming the other benchmarking control solutions.
- The control effort required by the CL-EMRAC solution is comparable to those provided by the benchmark controllers, as for most of the sub-maneuvers the control solutions have comparable IACA. Hence, the CL-EMRAC strategy is able to improve the closed-loop tracking performance without an excessive increase of the control effort.
- To evaluate the increase of computation complexity when the CL-EMRAC algorithm replaces the traditional CL-MRAC, the average simulation time and the average execution time of both controllers have been evaluated when the presented steering maneuver has been performed five times. Moreover, the computational platform used for simulating the control systems is an Intel Core i7-4700MQ 2.40 GHz processor and 16 GB RAM. Compared to the CL-MRAC algorithm, on the average the CL-EMRAC solution increased the simulation time of 9.7% while the execution time of the controller increased of 8.2%. These increases are acceptable considering the significant improvements of the KPIs measuring the tracking performance shown in Table 2 obtained when the CL-EMRAC algorithm is used instead of the classical CL-MRAC strategy.

6 | CONCLUSIONS

This article has presented the design and closed-loop analysis of a novel output-based closed-loop EMRAC algorithm. Lyapunov theory for smooth systems and Filippov systems has been adopted to study the convergence and ultimate boundedness of the closed-loop dynamics not only with respect to $\mathcal{L}_2$ disturbances but also for $\mathcal{L}_\infty$ unmodelled dynamics and disturbances. The novel output-based CL-EMRAC strategy has been applied to the direct yaw moment control problem, without the use of the vehicle sideslip angle information. The simulation analysis has been carried out through a high-fidelity IPG CarMaker model, and has shown that the CL-EMRAC solution is robust to the unmodelled vehicle dynamics, for example, the nonlinear tire characteristics and parameter mismatches. Moreover, the analysis of a set of KPIs has shown that: (*i*) the output-based CL-EMRAC strategy outperforms two full-state feedback LQ solutions and two MRAC strategies, used as benchmark controllers; and (*ii*) the adaptive switching and adaptive integral control actions of the CL-EMRAC are vital to enhance the ability of the closed-loop system to track the reference dynamics. Future study will explore the experimental validation of the proposed output-based CL-EMRAC solution, and its application to other automotive control problems, such as the stabilization of articulated vehicles.

ACKNOWLEDGMENTS

Deep thanks to the thoughtful comments from the Reviewers and Associate Editor which have improved the paper.

CONFLICT OF INTEREST

The authors declare no potential conflict of interests.

DATA AVAILABILITY STATEMENT

The data that support the findings of this study are available from the corresponding author upon reasonable request.

ORCID

Umberto Montanaro https://orcid.org/0000-0003-0620-1906
Chen Chen https://orcid.org/0009-0005-1047-4191
Alessandro Rizzo https://orcid.org/0000-0002-2386-3146

REFERENCES

1. Montanaro U, di Gaeta A, Giglio V. Robust discrete-time MRAC with minimal controller synthesis of an electronic throttle body. *IEEE/ASME Trans Mechatron*. 2014;19(2):524-537.
2. Buonomano A, Montanaro U, Palombo A, Santini S. Temperature and humidity adaptive control in multi-enclosed thermal zones under unexpected external disturbances. *Energ Buildings*. 2017;135:263-285.
3. Dixit S, Montanaro U, Dianati M, Mouzakitis A, Fallah S. Integral MRAC with bounded switching gain for vehicle lateral tracking. *IEEE Trans Control Syst Technol*. 2020;29(5):1936-1951.
4. Montanaro U, Martini S, Hao Z, Gao Y, Sorniotti A. Multi-input enhanced model reference adaptive control strategies and their application to space robotic manipulators. *Int J Robust Nonlinear Control*. 2023;33(10):5246-5272.
5. Landau YD. *Adaptive Control: The Model Reference Approach*. CRC Press; 1979.
6. Stepanyan V, Kalmanje K. MRAC revisited: guaranteed performance with reference model modification. *Proceedings of the 2010 American Control Conference*. IEEE; 2010:93-98.
7. Gibson TE, Qu Z, Annaswamy AM, Lavretsky E. Adaptive output feedback based on closed-loop reference models. *IEEE Trans Automat Contr*. 2015;60(10):2728-2733.
8. Xie J, Zhao J. H_∞ model reference adaptive control for switched systems based on the switched closed-loop reference model. *Nonlinear Anal Hybrid Syst*. 2018;27:92-106.
9. Xiao S, Dong J. Robust adaptive fault-tolerant tracking control for uncertain linear systems with actuator failures based on the closed-loop reference model. *IEEE Trans Syst Man Cybern Syst*. 2020;50(9):3448-3455.
10. Xiao S, Dong J. Output feedback adaptive fault-tolerant compensation tracking control for linear systems based on the closed-loop reference model. *Int J Adapt Control Signal Process*. 2020;34(1):77-91.
11. Goel R, Garg T, Roy S. Closed-loop reference model based distributed MRAC using cooperative initial excitation and distributed reference input estimation. *IEEE Trans Control Netw Syst*. 2022;9(1):37-49.
12. Huang X, Han X. Adaptive output-feedback resilient tracking control using virtual closed-loop reference model for cyber-physical systems with false data injection attacks. *Asian J Control*. 2022;25:1380-1391.
13. Liu Y, Yang J, Na J, Gao G, Wang S, Chen Q. Peaking reduction of CRM-based adaptive control via a modified adaptive law. *International Conference on Modelling, Identification and Control*. Springer; 2020:239-248.
14. Dey R, Jain SK, Padhy PK. Robust flexible adaptation gain based CRM for guaranteed transient performance. *Trans Inst Meas Control*. 2019;41(5):1233-1242.
15. Yuksek B, Inalhan G. Reinforcement learning based closed-loop reference model adaptive flight control system design. *Int J Adapt Control Signal Process*. 2021;35(3):420-440.
16. Ohrem SJ, Holden C. Adaptive controller and observer design using open and closed-loop reference models for linear time-invariant systems with unknown dynamics. *IEEE Trans Automat Contr*. 2021;66(11):5482-5489.
17. Zheng X, Yang X, Zhao H, Chen Y. Saturated adaptive-law-based backstepping and its applications to a quadrotor hover. *IEEE Trans Ind Electron*. 2022;69(12):13473-13482.
18. Khalil HK. *Nonlinear Systems*. 2nd ed. Prentice Hall; 2002.
19. Mu XW, Ding ZS, Cheng GF. Uniformly ultimate boundedness for discontinuous systems with time-delay. *Appl Math Mech*. 2011;32(9):1187-1196.
20. De Novellis L, Sorniotti A, Gruber P, et al. Direct yaw moment control actuated through electric drivetrains and friction brakes: theoretical design and experimental assessment. *Mechatronics*. 2015;26:1-15.
21. Sang N, Wei M. Adaptive control of active front steering and direct yaw moment for vehicle. *J Traffic Transp Eng*. 2016;16(3):91-99.
22. Ghezzi MK, Dòria-Cerezo A, Olm JM. Yaw moment MRAC with optimal torque vectoring for a four in-wheel motor EV. *2018 IEEE International Conference on Industrial Technology*. IEEE; 2018:1820-1825.
23. Ahmadian N, Khosravi A, Sarhadi P. Adaptive yaw stability control by coordination of active steering and braking with an optimized lower-level controller. *Int J Adapt Control Signal Process*. 2020;34(9):1242-1258.
24. Ahmadian N, Khosravi A, Sarhadi P. Managing driving disturbances in lateral vehicle dynamics via adaptive integrated chassis control. *Proc Inst Mech Eng K J Multi-Body Dyn*. 2021;235(1):122-133.
25. Li J, Ao D, Wang Y, Xiong R. Model reference adaptive stability control for independent driving electric vehicle. *J Automot Safety Energy*. 2021;12(3):355.
26. Jagga D, Lv M, Baldi S. Hybrid adaptive chassis control for vehicle lateral stability in the presence of uncertainty. *2018 26th Mediterranean Conference on Control and Automation (MED)*. IEEE; 2018:1-6.
27. Lenzo B, Sorniotti A, Gruber P. A single input single output formulation for yaw rate and sideslip angle control via torque-vectoring. 14th Symposium on Advanced Vehicle Control; 2018.
28. Zhou X, Wang Z, Shen H, Wang J. Yaw-rate-tracking-based automated vehicle path following: an MRAC methodology with a closed-loop reference model. *ASME Lett Dyn Syst Control*. 2022;2(2):021010.

29. Wang Z, Montanaro U, Fallah S, Sorniotti A, Lenzo B. A gain scheduled robust linear quadratic regulator for vehicle direct yaw moment control. *Mechatronics*. 2018;51:31-45.
30. Tao G. *Adaptive Control Design and Analysis*. John Wiley & Sons, Inc.; 2003.
31. Stoten DP, Benchoubane H. Robustness of a minimal controller synthesis algorithm. *Int J Control*. 1990;51(4):851-861.
32. Grant M, Boyd S, Ye Y. Disciplined convex programming. In: Liberti L, Maculan N, eds. *Global Optimization*. Nonconvex Optimization and its Applications. Springer; 2006:155-210.
33. Clarke FH. *Optimization and Nonsmooth Analysis*. Vol 5. SIAM; 1990.
34. Montanaro U, Olm JM. Integral MRAC with minimal controller synthesis and bounded adaptive gains: the continuous-time case. *J Franklin Inst*. 2016;353(18):5040-5067.
35. Cao Y, Sun Y, Cheng C. Delay dependent robust stabilization of uncertain systems with multiple state delays. *IEEE Trans Automat Contr*. 1999;43:1608-1612.
36. Shevitz D, Paden B. Lyapunov stability theory of nonsmooth systems. *IEEE Trans Automat Contr*. 1994;39(9):1910-1914.
37. di Bernardo M, Montanaro U, Ortega R, Santini S. Extended hybrid model reference adaptive control of piecewise affine systems. *Nonlinear Anal Hybrid Syst*. 2016;21:11-21.
38. Nakakuki T, Shen T, Tamura K. Adaptive control design for a class of nonsmooth nonlinear systems with matched and linearly parameterized uncertainty. *Int J Robust Nonlinear Control*. 2009;19:243-255.
39. Anderson BDO, Moore JB. *Optimal Control: Linear Quadratic Methods*. Prentice-Hall International; 1989.
40. Grant MC, Boyd SP. The CVX users' guide; 2020.
41. NHTSA. Electronic stability control systems. Technical report FMVSS No. 126. U.S. Department Of Transportation, National Highway Traffic Safety Administration; 2017.
42. Medina A, Bistue G, Rubio A. Comparison of typical controllers for direct yaw moment control applied on an electric race car. *Vehicles*. 2021;3:127-144.

How to cite this article: Montanaro U, Chen C, Rizzo A, Sorniotti A. Output-based enhanced closed-loop model reference adaptive control and its application to direct yaw moment control. *Int J Robust Nonlinear Control*. 2024;1-30. doi: 10.1002/rnc.7471

APPENDIX A. PROOF OF LEMMA 3

From Assumption 3, the matrix Q is strictly positive definite, thus, in accordance with the Schur complement, the matrix $\widetilde{Q}$ is positive if the matrix

$$\Xi = 2\theta C^T\Gamma_N HH^T\Gamma_N C - \frac{1}{\widehat{\phi}_R^2}C^T\Gamma_N H\widehat{\phi}_X^T Q^{-1}\widehat{\phi}_X H^T\Gamma_N C \tag{A1}$$

is positive.

By defining $z = H^T\Gamma_N C\chi \in \mathbb{R}$, with χ being a vector in $\mathbb{R}^{n_x}$, we have

$$\begin{aligned}\chi^T\Xi\chi > 0 \Leftrightarrow \quad & \chi^T\left(2\theta C^T\Gamma_N HH^T\Gamma_N C - \frac{1}{\widehat{\phi}_R^2}C^T\Gamma_N H\widehat{\phi}_X^T Q^{-1}\widehat{\phi}_X H^T\Gamma_N C\right)\chi > 0\\ \Leftrightarrow \quad & 2\theta z^2 - \frac{z^2}{\widehat{\phi}_R^2}\widehat{\phi}_X^T Q^{-1}\widehat{\phi}_X > 0 \Leftrightarrow 2\theta - \frac{1}{\widehat{\phi}_R^2}\widehat{\phi}_X^T Q^{-1}\widehat{\phi}_X > 0.\end{aligned} \tag{A2}$$

As

$$2\theta - \frac{1}{\widehat{\phi}_R^2}\widehat{\phi}_X^T Q^{-1}\widehat{\phi}_X > 2\theta - \lambda_{\max}\left(Q^{-1}\right)\frac{\left\|\widehat{\phi}_X\right\|^2}{\widehat{\phi}_R^2}, \tag{A3}$$

inequality (A2) is satisfied when the right-hand side of (A3) is made positive, which occurs when

$$\theta > \frac{\widehat{\phi}_{X,u}^2}{2\widehat{\phi}_{R,l}^2\lambda_{\min}(Q)} = \theta^\star. \tag{A4}$$

According to Assumption 3, θ is chosen greater than $\theta^\star$, thus inequality (A4) is satisfied and consequently Lemma 3 is proven.

APPENDIX B. PROOF OF LEMMA 4

In what follows it is shown that the matrix $-\Omega$ is strictly negative, that is, for any non null vector $z \in \mathbb{R}^{n_x}$, $-z^T\Omega z < 0$.

As Assumption 3 holds, the matrix $P(A_m + LC) + (A_m + LC)^T P$ can be upper bounded as in (66), thus

$$\begin{aligned} -z^T\Omega z &= z^T\left[P(A_m + LC) + (A_m + LC)^T P - \frac{2}{\widehat{\phi}_R} C^T\Gamma_N H\widehat{\phi}_X^T\right] z \\ &< -z^T\left[Q + 2\theta C^T\Gamma_N HH^T\Gamma_N C + \mathcal{I}_{n_x} + \frac{2}{\widehat{\phi}_R} C^T\Gamma_N H\widehat{\phi}_X^T\right] z = -z^T z - z_e^T\widetilde{Q} z_e, \end{aligned} \tag{B1}$$

where $z_e = \begin{bmatrix} z^T & z^T \end{bmatrix}^T$ and $\widetilde{Q}$ is the matrix in (47).

Now, according to Lemma 3, $\widetilde{Q}$ is positive, thus inequality (B1) can be further upper bounded as

$$-z^T\Omega z < -z^T z < 0, \tag{B2}$$

thus Ω is a strictly positive matrix.